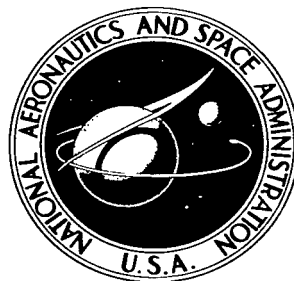


NASA TECHNICAL NOTE



NASA TN D-3692

C.1

NASA TN D-3692



THEORETICAL INVESTIGATION OF TURBULENT LIQUID-METAL HEAT TRANSFER IN CHANNELS WITH HEAT SOURCES IN THE FLUID

by Robert M. Inman
Lewis Research Center
Cleveland, Ohio





THEORETICAL INVESTIGATION OF TURBULENT LIQUID-METAL HEAT
TRANSFER IN CHANNELS WITH HEAT SOURCES IN THE FLUID

By Robert M. Inman

Lewis Research Center
Cleveland, Ohio

NATIONAL AERONAUTICS AND SPACE ADMINISTRATION

For sale by the Clearinghouse for Federal Scientific and Technical Information
Springfield, Virginia 22151 - Price \$2.50

THEORETICAL INVESTIGATION OF TURBULENT LIQUID-METAL HEAT TRANSFER IN CHANNELS WITH HEAT SOURCES IN THE FLUID

by Robert M. Inman
Lewis Research Center

SUMMARY

A previous analysis to determine the heat-transfer characteristics for turbulent flow of a heat-generating liquid metal in a parallel-plate channel (NASA TN D-3473) is extended by including the turbulent or eddy conductivity with the molecular conductivity as a means of transporting heat. The fully developed velocity distribution is taken as uniform, and an idealized eddy diffusivity function (obtained from Poppendiek) is used. Heat is generated uniformly in the flow, and the analysis is carried out for both uniform wall temperature and uniform wall heat flux. In solving the energy equation the factor $\bar{\psi}$, which is defined as the average effective value of the ratio of the eddy diffusivity of heat transfer to that of momentum transfer, is introduced. The analysis applies in the thermal entrance region of the channel as well as downstream.

The effects of the ratios of internal heat generation to wall heat transfer or temperature driving force on heat-transfer characteristics are investigated. Results for several quantities of engineering interest are presented as functions of the foregoing heat generation ratios, a dimensionless axial-distance modulus, and a parameter

$k = \sqrt{1 + 0.01 \bar{\psi} \text{PrRe}^{0.9}}$, where Pr is Prandtl number and Re is Reynolds number.

The solutions for Nusselt numbers are shown to reduce correctly to molecular-conduction heat-transfer results as k approaches unity. Results for the fully developed Nusselt numbers for liquid metal flow without internal heat sources are compared with existing calculations based on the assumption that the eddy diffusivities of heat and momentum ϵ_H and ϵ_M are equal and exhibit good agreement ($\bar{\psi} = \psi = 1$, where $\psi = \epsilon_H/\epsilon_M$). The present results apply to systems with Reynolds numbers ranging from 5000 to approximately 10^6 and Prandtl numbers ranging from 0.001 to 0.100.

INTRODUCTION

The following analysis is a sequel to an earlier formulation and analytical study of the problem of heat transfer to a liquid metal flowing between parallel plates with heat sources in the fluid stream (ref. 1). In that study the idealized system which defined turbulent heat transfer in a flowing liquid metal was based in part on the following postulates:

(1) The established turbulent velocity profile is represented by a uniform distribution (slug flow).

(2) The thermal eddy diffusivity is small compared to the thermal molecular diffusivity and is neglected (molecular conduction only).

The latter postulate implies that the thermal solutions obtained from this model pertain to systems characterized by low Prandtl and Reynolds numbers. These results will be referred to in this report as the molecular-conduction heat-transfer solutions.

The model to be developed in this report improves on the molecular conduction model by allowing for turbulent eddying within the liquid metal through the use of an idealized eddy diffusivity function (refs. 2 and 3). It is shown in references 2 and 3 that the idealized eddy diffusivity function approximates the actual one in the regions nearest the walls over a Reynolds number range of 5×10^3 to 1×10^6 . For symmetrical thermal boundary conditions, the use of this function should introduce little error, since the heat transfer is small in the central regions. For asymmetrical boundary conditions, however, a more realistic description may be necessary.

The assumption is also made in the development of the eddy diffusivity function in references 2 and 3 that the eddy diffusivities for momentum and heat are equal. Sufficient evidence now exists to indicate that, in general, ϵ_H and ϵ_M are not equal (refs. 4 to 10). (Symbols are defined in appendix A.) There is at present, however, no general agreement on the form and magnitude of the parameter ψ , defined as the ratio ϵ_H/ϵ_M . It is known that the term ψ varies across the flow channel as well as with both Prandtl and Reynolds numbers.

To eliminate the radial-dependence drawback, it is convenient (ref. 9) to introduce the parameter $\bar{\psi}$, which is the effective average value of ψ across the channel. When $\bar{\psi}$ is used, the problem of dealing with local variations in ψ is avoided. Reference 9 considers a method of evaluating the quantity $\bar{\psi}$ for practical use in estimating heat-transfer characteristics of turbulent, internal flow of liquid metals. The term $\bar{\psi}$ is introduced as a parameter in the present study. No attempt is made, however, to evaluate this quantity beyond assuming $\bar{\psi} = 1$ when comparing the present results with other theoretical predictions wherein the eddy diffusivities for momentum and heat are assumed equal.

The model postulated to approximate the forced convection heat-transfer system

under consideration is defined by the following assumptions:

- (1) The established turbulent velocity profile is represented by a uniform distribution $u(y) = U$.
- (2) Longitudinal heat conduction is small compared to convection and transverse heat conduction and therefore is neglected. This restriction is shown in reference 11 to introduce a negligible error for $RePr = Pe > 100$.
- (3) The eddy diffusivity of momentum distribution varies linearly with distance from the channel centerline and as the nine-tenths power of the Reynolds number:

$$\frac{\epsilon_M}{\nu} = 0.01 Re^{0.9} \left(1 - \frac{y}{a}\right)$$

- (4) The internal heat generation is spatially uniform.
- (5) The fluid properties are invariant with temperature.
- (6) A steady state exists.

The range of validity of this idealized model must be established primarily by comparison with existing numerical and experimental data. The present solutions reduce correctly to the molecular-conduction heat-transfer results for Nusselt numbers (ref. 1) as the eddy conduction contribution becomes negligible. The fully developed Nusselt numbers in the absence of internal heat generation are calculated on the basis of $\bar{\psi} = 1$ and compared with existing calculations (refs. 12 to 14) and shown to exhibit good agreement. Within the knowledge of the author, no heat-transfer measurements for turbulent liquid metal flows between parallel plates with heat sources in the fluid stream are available for comparison.

The present results are applicable in the design of liquid-metal-fuel reactors, electromagnetic pumps and flowmeters (e. g. , ref. 16), equipment for the electrolytic removal of gaseous impurities in liquid metals, and liquid metal magnetohydrodynamic power generators (e. g. , refs. 17 and 18).

GENERAL ANALYTICAL CONSIDERATIONS

A schematic diagram of the system under study is pictured in figure 1, which also shows dimensions and coordinates. The direction of fluid flow is from left to right. The section of the channel to the right of $x = 0$ is the region in which the fluid experiences a uniform internal heat generation Q and to which specific thermal boundary conditions are applied. Both uniform wall heat flux and uniform wall temperatures are considered. The fluid possesses a fully developed velocity profile which is unchanging with length. The temperature across the entrance section, $x = 0$, is taken to be uniform at

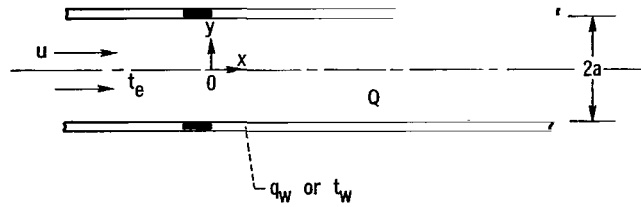


Figure 1. - Physical model and coordinates.

the value t_e . For each of the thermal situations, an analysis is carried out to determine the heat-transfer characteristics of the fluid at all positions along the duct, that is, in the thermal entrance as well as fully developed regions.

UNIFORM WALL HEAT FLUX

The starting point of the analysis is the equation expressing conservation of energy for turbulent liquid metal flow in a parallel-plate channel (often referred to as a flat duct). For fully developed hydrodynamic conditions, this equation may be written as

$$u \frac{\partial t}{\partial x} = \frac{\partial}{\partial y} \left[(\alpha + \epsilon_H) \frac{\partial t}{\partial y} \right] + \frac{Q}{\rho c_p} \quad (1)$$

where α and ϵ_H represent, respectively, the molecular and eddy diffusivities of heat. The turbulent velocity distribution is approximated by the uniform distribution

$$u(y) \equiv U = \text{constant} \quad (2)$$

Since equation (1) is linear in the temperature t , it is possible to separate the general problem, which includes both internal heat sources and wall heat transfer, into two simpler situations, which are: (1) a problem in which there is a uniform internal heat generation Q in the fluid flowing through a duct with insulated walls ($q_w = 0$) (for this case, the temperature is designated as t_Q) and (2) a problem in which there is a uniform heat transfer q_w at the channel walls but no internal heat generation ($Q = 0$) (in this instance the temperature is denoted by t_q). Then, from the linearity of the energy equation, the temperature in the combined problem is given by

$$t = t_Q + t_q \quad (3)$$

The governing equations and boundary conditions for t_Q and t_q may be written as follows:

$$U \frac{\partial t_Q}{\partial x} = \frac{\partial}{\partial y} \left[(\alpha + \epsilon_H) \frac{\partial t_Q}{\partial y} \right] + \frac{Q}{\rho c_p} \quad (4a)$$

$$\left. \begin{aligned} \frac{\partial t_Q}{\partial y} &= 0 \text{ at } y = a \text{ (insulated wall)} \\ \frac{\partial t_Q}{\partial y} &= 0 \text{ at } y = 0 \text{ (symmetry)} \\ t_Q &= 0 \text{ at } x = 0 \text{ (entrance condition)} \end{aligned} \right\} \quad (4b)$$

and

$$U \frac{\partial t_q}{\partial x} = \frac{\partial}{\partial y} \left[(\alpha + \epsilon_H) \frac{\partial t_q}{\partial y} \right] \quad (5a)$$

$$\left. \begin{aligned} \frac{\partial t_q}{\partial y} &= \frac{q_w}{\kappa} \text{ at } y = a \text{ (specified heat flux)} \\ \frac{\partial t_q}{\partial y} &= 0 \text{ at } y = 0 \text{ (symmetry)} \\ t_q &= t_e \text{ at } x = 0 \text{ (entrance condition)} \end{aligned} \right\} \quad (5b)$$

It is convenient to express equations (4) and (5) in terms of dimensionless variables defined in appendix A; then these equations are given as

$$\frac{\partial t_Q}{\partial x'} = \frac{\partial}{\partial y'} \left[\left(\frac{1}{Pr} + \frac{\epsilon_H}{\nu} \right) \frac{\partial t_Q}{\partial y'} \right] + \frac{Qa^2}{Pr\kappa} \quad (6a)$$

$$\left. \begin{aligned} \frac{\partial t_Q}{\partial y'} &= 0 \text{ at } y' = 0 \text{ and } y' = 1 \\ t_Q &= 0 \text{ at } x' = 0 \end{aligned} \right\} \quad (6b)$$

$$\frac{\partial t_q}{\partial x'} = \frac{\partial}{\partial y'} \left[\left(\frac{1}{Pr} + \frac{\epsilon_H}{\nu} \right) \frac{\partial t_q}{\partial y'} \right] \quad (7a)$$

$$\left. \begin{aligned} \frac{\partial t_q}{\partial y'} &= \frac{q_w a}{\kappa} \text{ at } y' = 1 \\ \frac{\partial t_q}{\partial y'} &= 0 \text{ at } y' = 0 \\ t_q &= t_e \text{ at } x' = 0 \end{aligned} \right\} \quad (7b)$$

It is noted that the dimensionless eddy diffusivity appears together with the reciprocal of the Prandtl number in the form of a sum

$$\begin{aligned} \frac{1}{Pr} + \frac{\epsilon_H}{\nu} &= \frac{1}{Pr} + \frac{\epsilon_H}{\epsilon_M} \frac{\epsilon_M}{\nu} \\ &= \frac{1}{Pr} + 0.01 \bar{\psi} Re^{0.9} (1 - y') \end{aligned} \quad (8)$$

This expression may be inserted into equations (6a) and (7a). The resulting equations can be expressed in a simpler form by making the change of variable,

$$r = \sqrt{F_0 + F_1(1 - y')} \quad (9)$$

where $F_0 = 1/Pr$ and $F_1 = 0.01 \bar{\psi} Re^{0.9}$. The heat-transfer problems to be solved then become

$$\frac{\partial t_Q}{\partial x'} = \frac{F_1^2}{4} \frac{1}{r} \frac{\partial}{\partial r} \left(r \frac{\partial t_Q}{\partial r} \right) + \frac{Qa^2}{Pr\kappa} \quad (10a)$$

$$\left. \begin{aligned} \frac{\partial t_Q}{\partial r} &= 0 \text{ at } r = r_0 \text{ and } r_1 \\ t_Q &= 0 \text{ at } x' = 0 \end{aligned} \right\} \quad (10b)$$



$$\frac{\partial t_q}{\partial x'} = \frac{F_1^2}{4} \frac{1}{r} \frac{\partial}{\partial r} \left(r \frac{\partial t_q}{\partial r} \right) \quad (11a)$$

$$\left. \begin{aligned} \frac{1}{r} \frac{\partial t_q}{\partial r} &= -\frac{2}{F_1} \frac{q_w a}{\kappa} \text{ at } r = r_1 \\ \frac{1}{r} \frac{\partial t_q}{\partial r} &= 0 \text{ at } r = r_0 \\ t_q &= t_e \text{ at } x' = 0 \end{aligned} \right\} \quad (11b)$$

where the limits are $r_0 = \sqrt{F_0 + F_1}$ and $r_1 = \sqrt{F_0}$. These equations complete the formulation of the boundary value problems. The two problems as defined by equations (10) and (11) will be analyzed separately.

The problem of a liquid metal with internal heat sources flowing in an insulated channel is considered first. Next, the results are obtained for the problem of uniform wall heat transfer with no heat sources. These solutions are then combined linearly to yield results for the general case of both internal heat sources and wall heat flux.

Internal Heat Generation in an Insulated Channel

A solution for the temperature distribution t_Q that satisfies the differential equation (10a) may be proposed as follows:

$$\left. \begin{aligned} t_Q &= \frac{Qa^2}{\kappa Pr} x' \\ &= \frac{Qa^2}{\kappa} x^+ \end{aligned} \right\} \quad (12)$$

where $x^+ = x'/Pr$. This form of solution also identically satisfies the entrance and boundary conditions given by equation (10b). Equation (12) is a solution of the given differential equation and satisfies all the entrance and boundary conditions. It is therefore concluded that the solution for t_Q that applies over the entire length of the channel is simply

$$\frac{t_Q}{Qa^2/\kappa} = x^+ \quad (13)$$

The local bulk fluid temperature $t_{Q,b}(x^+)$ along the channel length, for a uniform heat source, is given by

$$\rho U c_p [t_{Q,b}(x^+) - t_{Q,b}(0)] = Qx$$

or, since $t_{Q,b}(0) = 0$,

$$t_{Q,b} = \frac{Qa^2}{\kappa} x^+ \quad (14)$$

Uniform Wall Temperature Without Internal Heat Generation

There is considered next the situation where there is heat transfer q_w at the channel walls but no internal heat generation.

For uniform wall heating conditions, it is known that, as the flow proceeds farther and farther down the channel, the heat-transfer characteristics asymptotically approach a limiting condition. This limit is termed the fully developed heat-transfer situation and will be denoted by the subscript d . It is convenient to write the temperature distribution t_q as the sum

$$t_q = t_{q,d} + t_q^* \quad (15)$$

Then t_q^* is seen to be an entrance region temperature that is added to $t_{q,d}$ to obtain temperatures in the region near the entrance of the channel and that approaches zero as x becomes large.

Fully Developed Solution

Since energy conservation must everywhere be satisfied, it is necessary that $t_{q,d}$ satisfy equation (11a); that is,

$$\frac{\partial t_{q,d}}{\partial x'} = \frac{F_1^2}{4} \frac{1}{r} \frac{\partial}{\partial r} \left(r \frac{\partial t_{q,d}}{\partial r} \right) \quad (16)$$

A characteristic of the fully developed situation for uniform wall heat transfer is that the temperature at all points in the cross section rises linearly along the channel. From a heat balance on the fluid, it follows that the temperature gradient in the fully developed region must be

$$\frac{\partial t_{q,d}}{\partial x} = \frac{q_w}{\rho U c_p a} \quad (17a)$$

or alternately

$$\frac{t_{q,d} - t_{q,e}}{q_w a / \kappa} = x' + G(r) \quad (17b)$$

The radial distribution $G(r)$ must, of course, satisfy the conservation-of-energy equation (16). When equation (17b) is substituted into equation (16), the governing equation for $G(r)$ is found to be

$$\frac{1}{r} \frac{d}{dr} \left(r \frac{dG}{dr} \right) = \frac{4}{Pr F_1^2} \quad (18a)$$

The boundary conditions on $G(r)$ are found from equations (11b) to be given by

$$\left. \begin{aligned} \frac{dG}{dr} &= 0 \quad \text{at } r = r_0 \\ \frac{dG}{dr} &= -\frac{2}{F_1} \quad \text{at } r = r_1 \end{aligned} \right\} \quad (18b)$$

The consideration of an overall energy balance on the fluid for the length of channel from 0 to x ,

$$\int_0^1 [t_{q,d}^{(x)} - t_e] dy' = \frac{q_w x}{\rho U c_p a}$$

leads to an additional condition, upon substitution of equation (17b), on $G(r)$ as

$$\int_{r_0}^{r_1} r G(r) dr = 0 \quad (18c)$$

Equation (18a) can be integrated directly. The resulting expression for $G(r)$ is

$$G(r) = \frac{2F_0}{F_1^2} \left(\frac{1}{2} r^2 - r_0^2 \ln r \right) + \frac{2F_0(F_0 + F_1)}{F_1^2} \left[\ln \left(\sqrt{F_0 + F_1} \right) - 1 + \frac{F_0}{F_1} \ln \left(\sqrt{1 + \frac{F_1}{F_0}} \right) \right] + \frac{F_0}{2F_1} \quad (19)$$

The expression for the fully developed temperature distribution is then given by equations (17b) and (19).

Thermal Entrance Region

According to equation (15), the temperature distribution in the thermal entrance region is found by adding the difference temperature t_q^* to the fully developed temperature $t_{q,d}$. Since $t_{q,d}$ has been determined, attention is turned to t_q^* . From the linearity of the energy equation, the equation for t_q^* must be

$$\frac{\partial t_q^*}{\partial x'} = \frac{F_1^2}{4} \frac{1}{r} \frac{\partial}{\partial r} \left(r \frac{\partial t_q^*}{\partial r} \right) \quad (20a)$$

Since the wall heat addition has already been accounted for in the fully developed solution, the boundary conditions for t_q^* are given by

$$\frac{\partial t_q^*}{\partial r} = 0 \quad \text{at } r = r_0 \quad \text{and } r = r_1 \quad (20b)$$

and

or

$$\left. \begin{aligned} t_q^* &= t_e - t_{q,d} \\ \frac{t_q^*}{q_w a/\kappa} &= -G(r) \end{aligned} \right\} \text{at } x' = 0 \quad (20c)$$

where equation (17b) has been used in finding the last expression.

A solution for t_q^* is sought in the form of a product

$$\frac{t_q^*}{q_w a/\kappa} = \theta(r)\tau(x') \quad (21)$$

where τ and θ , respectively, depend on x' and r alone. Substituting equation (21) into the differential equation (20a) results in two total differential equations. One involves $\tau(x')$ and the other $\theta(r)$. The solution of these equations yields

$$\frac{t_q^*}{q_w a/\kappa} = e^{-\bar{\beta}^2 x'} \left[c_1 J_0 \left(\frac{2\bar{\beta}}{F_1} r \right) + c_2 Y_0 \left(\frac{2\bar{\beta}}{F_1} r \right) \right] \quad (22)$$

where $\bar{\beta}$ is the separation constant arising from the product solution, and c_1 and c_2 are constants in the general solution.

From the boundary condition $\partial t_q^* / \partial r = 0$ at $r = r_0$, the constant c_1 is

$$c_1 = -c_2 \frac{Y_1 \left(\frac{2\bar{\beta}}{F_1} r_0 \right)}{J_1 \left(\frac{2\bar{\beta}}{F_1} r_0 \right)} \quad (23)$$

Hence the solution for t_q^* can be written as

$$\begin{aligned}
\frac{t_q^*}{q_w a / \kappa} &= \frac{c_2 e^{-\bar{\beta}^2 x'}}{J_1\left(\frac{2\bar{\beta}}{F_1} r_0\right)} \left[-Y_1\left(\frac{2\bar{\beta}}{F_1} r_0\right) J_0\left(\frac{2\bar{\beta}}{F_1} r\right) + J_1\left(\frac{2\bar{\beta}}{F_1} r_0\right) Y_0\left(\frac{2\bar{\beta}}{F_1} r\right) \right] \\
&= \frac{c_2 e^{-\bar{\beta}^2 x'}}{J_1\left(\frac{2\bar{\beta}}{F_1} r_0\right)} V_0\left(\frac{2\bar{\beta}}{F_1} r\right)
\end{aligned} \tag{24}$$

The constant $\bar{\beta}$ can be evaluated by substituting equation (24) into the boundary condition $\partial t_q^* / \partial r = 0$ at $r = r_1$. The solution comprises an eigenvalue problem of the Sturm-Liouville type. Solutions fitting this boundary condition can be found only for discrete values of $\bar{\beta}$, that is, $\bar{\beta}_1, \bar{\beta}_2, \dots, \bar{\beta}_m$, termed eigenvalues. The solutions $V_0[(2\bar{\beta}_1/F_1)r], \dots, V_0[(2\bar{\beta}_m/F_1)r]$ are the corresponding eigenfunctions. The eigenvalues $\bar{\beta}_m$ are found to be the positive roots of

$$J_1(w_m) Y_1(kw_m) - Y_1(w_m) J_1(kw_m) = 0 \tag{25}$$

where $w_m = (2r_1/F_1)\bar{\beta}_m$ and k is a dimensionless diffusivity parameter defined as

$$\begin{aligned}
k &= \frac{r_0}{r_1} = \sqrt{\frac{F_0 + F_1}{F_0}} \\
&= \sqrt{1 + 0.01 \bar{\psi} \text{PrRe}^{0.9}}
\end{aligned} \tag{26}$$

The first five values of the roots w_m are given in reference 19 for several values of the parameter k . It is clear that the product $\bar{\psi} \text{PrRe}^{0.9}$ can never be negative, since negative values of $\bar{\psi}$ and/or negative Prandtl and Reynolds numbers are physically impossible. Therefore, k is equal to or greater than unity for all physically possible values of $\bar{\psi}$, Pr, and Re. It follows from equation (26) that the particular value $k = 1$ corresponds to molecular conduction and is interpreted to result for $\text{Pr} \rightarrow 0$.

The first five eigenvalues $\beta_m^2 = \bar{\beta}_m^2 / F_0 = w_m^2 (k^2 - 1)^2 / 4$ have been computed from the tabulations given in reference 19 for values of k of 1.25, 1.67, 2.50, and 5.00. An analysis of the eigenvalues β_m^2 for $k = 1$ has been given in reference 1 with the result

TABLE I. - LISTING OF EIGENVALUES β_m^2

Diffusivity parameter, k	Eigenvalue				
	β_1^2	β_2^2	β_3^2	β_4^2	β_5^2
1.00	9.872	39.48	88.83	158.0	246.8
1.25	12.56	49.99	112.6	200.0	312.4
1.67	17.89	70.55	158.2	281.1	439.4
2.50	32.03	122.9	274.2	485.8	758.2
5.00	103.3	373.7	819.8	1442	2242

$$\beta_m^2 (k = 1) = (m\pi)^2; m = 1, 2, \dots \quad (27)$$

The eigenvalues are listed in table I for the k values previously mentioned.

The constants c_2 in equation (24) are replaced by the coefficients a_m corresponding to the eigenvalues β_m^2 ; hence the solution for t_q^* can be written as

$$\begin{aligned} \frac{t_q^*}{q_w a/k} &= \sum_{m=1}^{\infty} \frac{a_m}{J_1(kw_m)} V_0\left(w_m \frac{r}{r_1}\right) e^{-\beta_m^2 x^+} \\ &= \sum_{m=1}^{\infty} A_m V_0\left(w_m \frac{r}{r_1}\right) e^{-\beta_m^2 x^+} \end{aligned} \quad (28)$$

where

$$A_m = \frac{a_m}{J_1(kw_m)} \quad (29)$$

and

$$V_0\left(w_m \frac{r}{r_1}\right) = -Y_1(kw_m)J_0\left(w_m \frac{r}{r_1}\right) + J_1(kw_m)Y_0\left(w_m \frac{r}{r_1}\right) \quad (30)$$

The coefficients A_m of equation (28) remain to be determined. When the boundary condition at the channel entrance as given by equation (20c) is applied, there is obtained

$$\sum_{m=1}^{\infty} A_m V_0\left(w_m \frac{r}{r_1}\right) = -G(r) \quad (31a)$$

and it follows immediately, from the properties of the Sturm-Liouville system for orthog-

onal functions, that the coefficients A_m are given by

$$A_m = - \frac{\int_{r_0}^{r_1} r G(r) V_0 \left(w_m \frac{r}{r_1} \right) dr}{\int_{r_0}^{r_1} r V_0^2 \left(w_m \frac{r}{r_1} \right) dr} \quad (31b)$$

where $G(r)$ is given by equation (19) and $V_0 \left(w_m \frac{r}{r_1} \right)$ satisfies the differential equation

$$\frac{1}{r} \frac{d}{dr} \left(r \frac{dV_0}{dr} \right) + \frac{w_m^2}{r_1^2} V_0 = 0 \quad (32)$$

The analytical evaluation of the coefficients A_m has been carried out in detail in appendix B with the result

$$A_m = \frac{4V_0(w_m)}{w_m^2(k^2 - 1) [V_0^2(w_m) - k^2 V_0^2(kw_m)]} \quad (33)$$

It will be useful, in the subsequent analysis, to introduce a new coefficient \bar{A}_m , defined as the product $A_m V_0(w_m)$:

$$\bar{A}_m = \frac{4V_0^2(w_m)}{w_m^2(k^2 - 1) [V_0^2(w_m) - k^2 V_0^2(kw_m)]} \quad (34a)$$

TABLE II. - VALUES OF COEFFICIENTS \bar{A}_m

Diffusivity parameter, k	Coefficient				
	$-\bar{A}_1$	$-\bar{A}_2$	$-\bar{A}_3$	$-\bar{A}_4$	$-\bar{A}_5$
1.00	0.20258	0.05066	0.02251	0.01266	0.00810
1.25	.17870	.04494	.02000	.01125	.00721
1.67	.14543	.03756	.01680	.00947	.00607
2.50	.09969	.02771	.01261	.00715	.00460
5.00	.04165	.01408	.00684	.00400	.00261

The coefficients \bar{A}_m for the particular case $k = 1$ are evaluated in reference 1 and given as

$$\bar{A}_m = -\frac{2}{(m\pi)^2}, \quad k = 1 \quad (34b)$$

Numerical values of \bar{A}_m are listed in table II as a function of the values

of k previously mentioned.

With the β_m , $V_0\left(w_m \frac{r}{r_1}\right)$, and A_m determined, the difference temperature, t_q^* , is then known from equation (28). It is now possible to proceed with the complete solution of the problem.

Complete Solution

The solution for the temperature t_q that applies in both the entrance and fully developed regions is found by summing the solutions for $t_{q,d}$ and t_q^* to yield the result

$$\frac{t_q - t_e}{q_w a / \kappa} = x^+ + G(r) + \sum_{m=1}^{\infty} A_m V_0\left(w_m \frac{r}{r_1}\right) e^{-\beta_m^2 x^+} \quad (35)$$

The local bulk fluid temperature $t_{q,b}$ in the presence of uniform wall heat transfer is given by

$$\rho U c_p a [t_{q,b}(x) - t_e] = q_w x$$

or alternately

$$\frac{t_{q,b} - t_e}{q_w a / \kappa} = x^+ \quad (36)$$

Combined Internal Sources and Wall Heat Transfer

The solution for the situation where internal heat generation and wall heat transfer occur simultaneously can now be written. According to equation (3), the result for this combined problem is found by adding the contributions due to each of the separate problems to obtain

$$t - t_e = \left(\frac{Qa^2}{\kappa} + \frac{q_w a}{\kappa}\right) x^+ + \frac{q_w a}{\kappa} G(r) + \frac{q_w a}{\kappa} \sum_{m=1}^{\infty} A_m V_0\left(w_m \frac{r}{r_1}\right) e^{-\beta_m^2 x^+} \quad (37a)$$

or in dimensionless form,

$$\frac{t - t_e}{q_w a / \kappa} = (1 + R)x^+ + G(r) + \sum_{m=1}^{\infty} A_m V_0 \left(w_m \frac{r}{r_1} \right) e^{-\beta_m^2 x^+} \quad (37b)$$

where

$$R = \frac{Qa}{q_w} \quad (38)$$

The heat-flux parameter R is the ratio of internal heat generation to the heat transferred at the channel walls and gives a measure of the relative importance, in connection with temperature development, of internal heat evolution in the presence of wall heat transfer.

Of particular practical interest is the wall temperature variation corresponding to uniform wall heat transfer and internal heat generation. This quantity can be found from equation (37b) by evaluating the equation at $r = r_1$:

$$\frac{t_w - t_e}{q_w a / \kappa} = (1 + R)x^+ + G(r_1) + \sum_{m=1}^{\infty} A_m e^{-\beta_m^2 x^+} \quad (39)$$

where $G(r_1)$ is given by

$$G(r_1) = \frac{2F_0}{F_1^2} \left(\frac{1}{2} r_1^2 - r_0^2 \ln r_1 \right) + \frac{2F_0(F_0 + F_1)}{F_1^2} \left[\ln \left(\sqrt{F_0 + F_1} \right) - 1 + \frac{F_0}{F_1} \ln \left(\sqrt{1 + \frac{F_1}{F_0}} \right) \right] + \frac{F_0}{2F_1} \quad (40a)$$

Equation (40a) can be recast to better reveal the sole dependence on the parameter $k = \sqrt{1 + 0.01 \bar{\psi} Pr Re}^{0.9}$. After considerable algebraic manipulation the alternative expression for $G(r_1)$ is given by

$$G(r_1) = \frac{2k^4 \ln k - k^2(k^2 - 1) - \frac{1}{2}(k^2 - 1)^2}{(k^2 - 1)^3} \equiv G(k) \quad (40b)$$

A convenient alternate form of equation (39) is obtained by introducing the local bulk fluid temperature t_b . The bulk temperature for the situation of combined uniform heat generation and wall heating is computed from

$$t_b(x^+) = t_e + \left(\frac{q_w a}{\kappa} + \frac{Qa^2}{\kappa} \right) x^+$$

or alternately

$$\frac{t_b - t_e}{q_w a / \kappa} = (1 + R)x^+ \quad (41)$$

Then the difference between the wall and bulk temperatures at all stations along the channel is given by

$$\frac{t_w - t_b}{q_w a / \kappa} = G(k) + \sum_{m=1}^{\infty} A_m e^{-\beta_m^2 x^+} \quad (42)$$

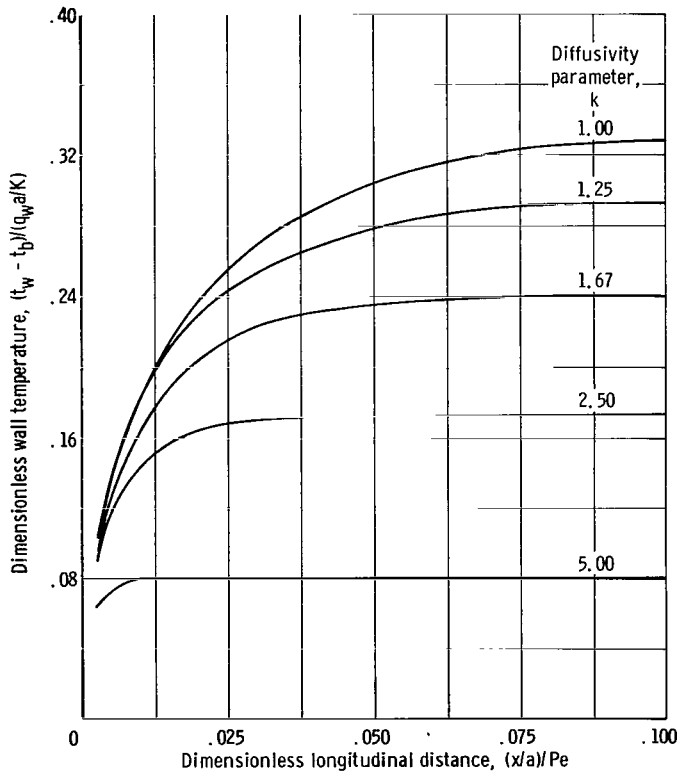


Figure 2. - Wall temperature results for internal heat generation with wall heat transfer.

A noteworthy feature of equation (42) is that the variation of the local wall-to-bulk-temperature differences is independent of the internal heat generation rate.

The longitudinal variations of the dimensionless wall temperatures were evaluated from the analytical solution (eq. (42)), and the results are plotted in figure 2. In interpreting this figure, it is important to note that the Reynolds and Prandtl numbers appear both in the parameter k and in the abscissa. The information given in this plot permits evaluation of the wall-to-bulk-temperature at various stations along the channel.

The fact that the temperature dif-

ference $t_w - t_b$ (eq. (42)) at any axial location is independent of the heat-flux ratio R is believed due primarily to the assumptions of a uniform velocity distribution and constant physical properties. This is only conjecture, of course, and further investigation would be required to support any definitive conclusion. It is worth mentioning, however, that the effect of an internal heat source on the fully developed heat-transfer coefficient for turbulent flow in a pipe with uniform wall heating has been investigated (ref. 20). For flow with a one-seventh power-law velocity distribution and $Pr = 0$, it is concluded in reference 20 that in general the influence of an internal source on the heat transfer coefficient (and thus on the temperature difference $t_w - t_b$) is slight. It therefore would appear that the influence of an internal source on $t_w - t_b$ would be slight at all axial locations, even for $Pr > 0$, and hence the assumption of slug flow, for example, does not introduce a serious error. Again this is only conjecture and should not be considered as fact.

Another quantity which is of practical interest is the fluid bulk temperature variation along the length of the channel. The bulk temperature is given relative to the temperature of the fluid at the entrance to the channel. The dimensionless bulk temperature given by equation (41) has been plotted in figure 3 for parametric values of the heat-flux parameter R .

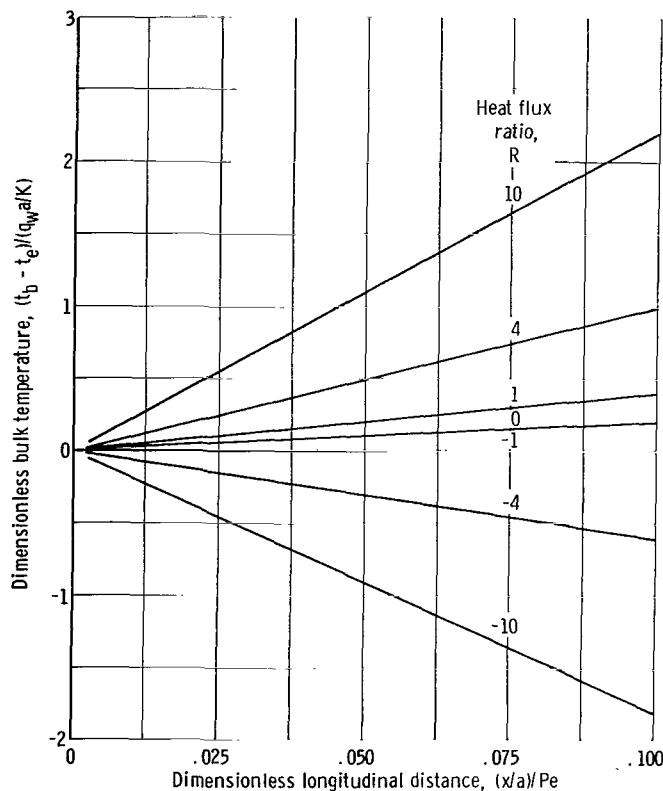


Figure 3. - Bulk temperature results for internal heat generation with wall heat transfer.

Positive and negative values of the parameter R are considered in the figures. In the present analysis Q is taken to be positive (a heat source). A positive value of R , therefore, implies that q_w is positive, or that heat is being transferred from the walls to the fluid. A negative value of R , on the other hand, implies that q_w is negative, or that heat is being transferred from the fluid to the walls. For a positive R , therefore, internal heat generation and wall heat transfer reinforce one another to produce a bulk temperature larger than that obtained in the absence of internal heat generation. Conversely, for a negative R , the wall heat transfer opposes internal heat generation in the bulk temperature development.

The wall-to-bulk-temperature dif-

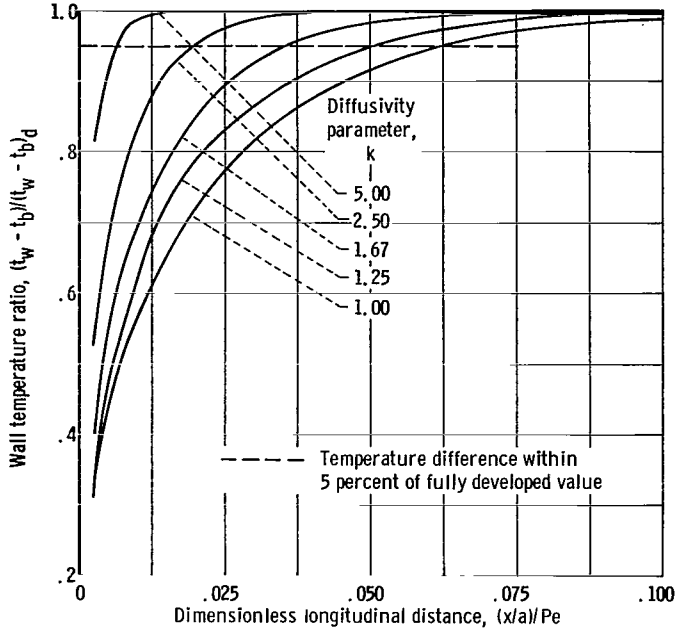


Figure 4. - Wall temperature ratio in thermal entrance region for internal heat generation with wall heat transfer.

ference for the fully developed situation ($x \rightarrow \infty$) is found from equation (42) to be

$$\frac{(t_w - t_b)_d}{q_w a / \kappa} = G(k) \quad (43)$$

A convenient rephrasing of equation (42) may then be carried out by introducing the fully developed wall-to-bulk-temperature difference, which yields

$$\frac{t_w - t_b}{(t_w - t_b)_d} = 1 + \frac{\sum_{m=1}^{\infty} \bar{A}_m e^{-\beta_m^2 x^+}}{G(k)} \quad (44)$$

The ratio of temperature differences is plotted in figure 4 as a function of the dimensionless axial distance along the channel for parametric values of k by using the numerical data listed in tables I and II. Thermal entrance length is commonly defined as the heated length required for $t_w - t_b$ to approach to within 5 percent of the fully developed value. A dashed line is drawn in figure 4 to facilitate finding the entrance length. For example, for $\bar{\psi} = 1$, for $Re = 56\ 000$, and $Pr = 0.003$ ($Pe = 168$ and $k = 1.25$), the dimensionless entrance length x/a is approximately 8, while for $Re = 672\ 000$ and the same Prandtl number, $Pr = 0.003$ ($Pe = 2015$ and $k = 2.50$), the entrance length x/a is approximately 38. Therefore, the entrance length (for $\bar{\psi} = 1$) increases as the Reynolds number increases.

It is customary to represent heat-transfer results in terms of a heat-transfer coefficient $h \equiv q_w / (t_w - t_b)$ and a Nusselt number $Nu \equiv h D_H / \kappa$, where D_H is the hydraulic diameter ($D_H = 4a$ for the parallel-plate channel). With these definitions, it follows from equation (42) that the Nusselt number is given by

$$Nu = \frac{4}{G(k) + \sum_{m=1}^{\infty} \bar{A}_m e^{-\beta_m^2 x^+}} \quad (45)$$

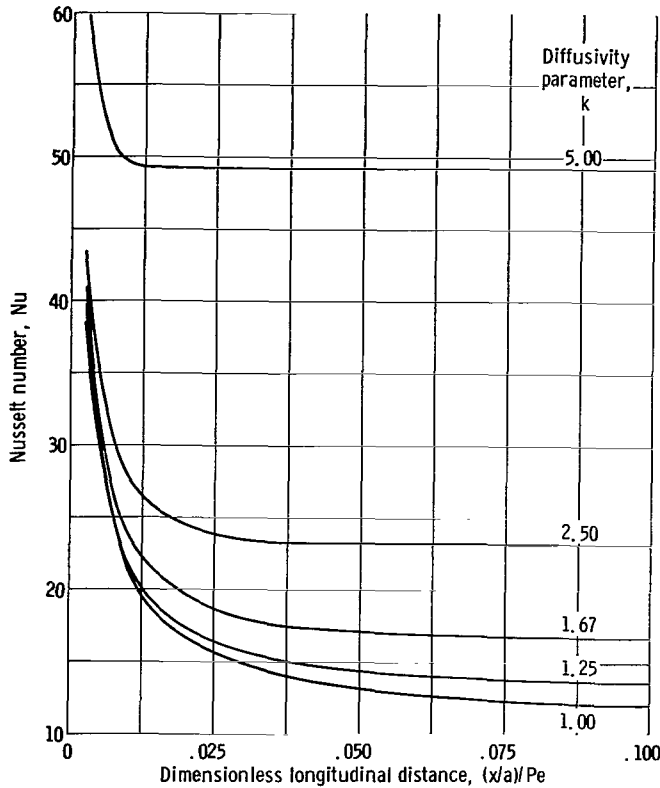


Figure 5. - Nusselt number results for internal heat generation with wall heat transfer.

Numerical values of the Nusselt number have been evaluated as a function of the dimensionless axial distance $x^+/4$ and the diffusivity parameter k and are plotted in figure 5. The information given in this plot permits rapid evaluation of the heat-transfer coefficient along the length of the duct.

It is of practical interest to examine the Nusselt number in the fully developed region Nu_d . This is obtained from equation (45) by considering the limit $x^+ \rightarrow \infty$:

$$Nu_d = \frac{4}{G(k)}$$

$$= \frac{4(k^2 - 1)^3}{2k^4 \ln k - k^2(k^2 - 1) - \frac{1}{2}(k^2 - 1)^2}$$

(46a)

Equation (46a) for the limiting case $k = 1$ assumes the indeterminate form $0/0$. Hence, it is necessary to apply L'Hospital's rule and to differentiate numerator and denominator with respect to k before setting $k = 1$. Repeated application of this rule yields the final result

$$Nu_d = 12 \quad (k = 1) \quad (46b)$$

This result agrees with that given in reference 1 for molecular-conduction heat transfer. It should be noted that equations (46a) and (46b) are independent of the internal heat generation rate.

The foregoing results are illustrated in figure 6, where the fully developed Nusselt number Nu_d is plotted as a function of the parameter k . Analytical data from reference 13 for fully developed Nusselt numbers employing velocity-profile and eddy diffusivity of momentum ϵ_M correlations, and data from reference 14 for fully developed Nusselt numbers employing experimentally determined velocity profile and friction factor correlations also appear in figure 6. The velocity-profile correlations used in calculat-

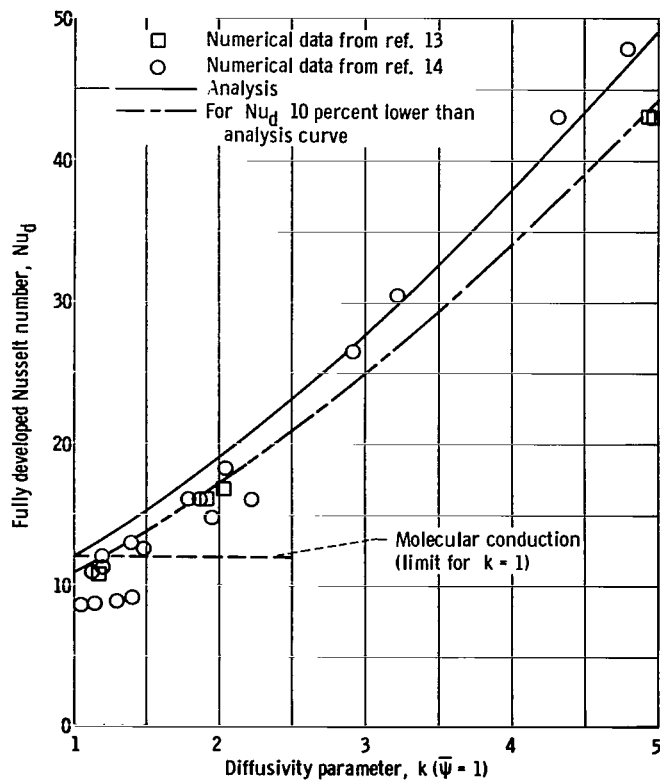


Figure 6. - Fully developed Nusselt number results for wall heat transfer and no internal heat sources. Average eddy diffusivity ratio, 1.

ing eddy diffusivities and Nusselt numbers in reference 13 were based upon experimental results of several investigators. In addition, the tabulated Nusselt numbers (which apply only for uniform wall heat flux and no heat sources) were calculated in reference 13 on the basis of $\epsilon_H = \epsilon_M$ and were obtained with the aid of a digital computer.

The Reynolds and Prandtl numbers to which the Nusselt numbers in reference 13 correspond were converted to the equivalent values of the parameter k (calculated for $\bar{\psi} = \psi = 1$). The results are presented for comparison in figure 6. The Reynolds numbers ranged from approximately 12 500 to 1.35×10^6 with a corresponding range in Péclet numbers from approximately 100 to 10^4 .

The calculated results presented by Martinelli in the discussion section of reference 14 represent corrected values of the Nusselt numbers previously presented by Martinelli in reference 12. In these calculations, experimentally determined velocity-profile and friction-factor correlations were used, as mentioned previously. A value of $\epsilon_H/\epsilon_M = 1.00$ was also employed in the numerical computations. The tabulated values listed in reference 14 are for Prandtl numbers ranging from 0 to 1.0 for Reynolds numbers from 2000 to 10^7 . However, only values in the Prandtl number range 0.001 to 0.100 for Reynolds numbers from 2000 to 10^6 were considered here for comparison.

It can be seen from figure 6 that equation (46a) gives results which are only approximately 10 percent greater than the fully developed Nusselt values given in reference 13 over the range of k values shown. The inclusion of a slightly more realistic velocity profile in the present study might decrease this difference, but further study is necessary before a real conclusion can be drawn. The present analysis for values of k greater than 3.0 is in good agreement with the numerical data of reference 14. For k less than 3.0, the analysis overestimates these numerical data by approximately 10 percent.

The author knows of neither analytical results including the effect of heat sources nor experimental results for heat transfer to liquid metals containing heat sources and

flowing turbulently between parallel plates that would allow for quantitative comparison with the present model. However, from consideration of the limiting solutions and comparison with existing calculations, it appears that the present relations are reasonably correct and can be used to calculate the heat-transfer design characteristics over the entire length of the passage for the Reynolds number range from 5000 to approximately 10^6 .

UNIFORM WALL TEMPERATURE

Consideration is now given to the problem where a liquid metal at a uniform temperature t_e enters a channel whose walls are maintained at a uniform temperature t_w , different from the entrance value (fig. 1, p. 4). In addition, a uniform heat generation begins in the fluid at $x = 0$. The starting point for the uniform wall temperature problem is also the energy conservation equation (1), and the velocity profile is again represented by equation (2).

Because of the linearity of the energy equation, it is again possible to write the fluid temperature $t(x, y)$ as the sum of two parts,

$$t(x, y) = t_Q(x, y) + t_T(x, y) \quad (47a)$$

where t_Q corresponds to the problem in which a heat-generating liquid metal at $t = 0$ enters a channel whose wall temperatures are also $t = 0$ and t_T corresponds to the problem in which a nongenerating liquid metal at t_e enters a channel whose wall temperatures are t_w . It will prove convenient to rewrite equation (47a) in the dimensionless form

$$\frac{t(x, y) - t_w}{t_e - t_w} = \frac{t_Q(x, y)}{t_e - t_w} + \frac{t_T(x, y) - t_w}{t_e - t_w}$$

or

$$T \equiv T_Q + T_T \quad (47b)$$

The dimensionless governing equations and boundary conditions for T_Q and T_T are

$$\frac{\partial T_Q}{\partial x'} = \frac{F_1^2}{4} \frac{1}{r} \frac{\partial}{\partial r} \left(r \frac{\partial T_Q}{\partial r} \right) + \frac{Qa^2}{\kappa Pr(t_e - t_w)} \quad (48a)$$

$$\left. \begin{aligned} \frac{\partial T_Q}{\partial r} &= 0 \text{ at } r = r_0 \\ T_Q &= 0 \text{ at } r = r_1 \\ T_Q &= 0 \text{ at } x' = 0 \end{aligned} \right\} \quad (48b)$$

and

$$\frac{\partial T_T}{\partial x'} = \frac{F_1^2}{4} \frac{1}{r} \frac{\partial}{\partial r} \left(r \frac{\partial T_T}{\partial r} \right) \quad (49a)$$

$$\left. \begin{aligned} \frac{\partial T_T}{\partial r} &= 0 \text{ at } r = r_0 \\ T_T &= 0 \text{ at } r = r_1 \\ T_T &= 1 \text{ at } x' = 0 \end{aligned} \right\} \quad (49b)$$

The solution proceeds in the same manner as for the uniform wall-heat-flux case; that is, the two problems are treated separately and the results are then combined to yield information for the general situation. For each problem the fully developed situation is considered first and then a difference-temperature, applicable in the entrance region, is dealt with. These solutions are then superposed.

Internal Heat Generation With Wall Temperature of Zero

Fully developed solution. - In the fully developed region the fluid flows isothermally ($\partial t_{Q,d}/\partial x = 0$) and therefore from equation (48a) $t_{Q,d}$ satisfies the equation

$$\frac{1}{r} \frac{\partial}{\partial r} \left(r \frac{\partial T_{Q,d}}{\partial r} \right) = -\frac{4}{F_1^2} \frac{Qa^2}{\kappa \text{Pr}(t_e - t_w)} \quad (50a)$$

with the boundary conditions

$$\left. \begin{aligned} \frac{\partial T_{Q,d}}{\partial r} &= 0 \text{ at } r = r_0 \\ T_{Q,d} &= 0 \text{ at } r = r_1 \end{aligned} \right\} \quad (50b)$$

Equation (50a) may be integrated directly. The resulting expression for $T_{Q,d}$ is

$$T_{Q,d} = \frac{2}{F_1^2} \frac{Qa^2}{\kappa \text{Pr}(t_e - t_w)} \left[r_0^2 \ln\left(\frac{r}{r_1}\right) - \frac{r^2 - r_1^2}{2} \right] \quad (51)$$

To determine the solution in the thermal entrance region, an entrance temperature T_Q^* is introduced such that

$$T_Q^* = T_Q - T_{Q,d} \quad (52)$$

Since $T_{Q,d}$ has already been determined attention is now turned to T_Q^* .

Entrance region solution. - To find the governing equation for T_Q^* , equation (52) is introduced into the energy conservation equation (48a). Since $T_{Q,d}$ satisfies equation (50a), it follows that T_Q^* must obey

$$\frac{\partial T_Q^*}{\partial x'} = \frac{F_1^2}{4} \frac{1}{r} \frac{\partial}{\partial r} \left(r \frac{\partial T_Q^*}{\partial r} \right) \quad (53a)$$

The boundary conditions on T_Q^* may be derived from equation (48a), in conjunction with equation (52), with the results

$$\left. \begin{aligned} \frac{\partial T_Q^*}{\partial r} &= 0 \text{ at } r = r_0 \\ T_Q^* &= 0 \text{ at } r = r_1 \end{aligned} \right\} \quad (53b)$$

and

$$\left. \begin{aligned} T_Q^* &= -T_{Q,d} \\ &= -\frac{2}{F_1^2} \frac{Qa^2}{\kappa \text{Pr}(t_e - t_w)} g(r) \end{aligned} \right\} \text{at } x' = 0 \quad (53c)$$

where $g(r) = r_0^2 \ln(r/r_1) - (1/2)(r^2 - r_1^2)$.

The solution of equation (53a) that will satisfy equations (53b) and (53c) can be found by using a product solution that leads to a separation of variables. This will have the form

$$T_Q^* = \frac{2}{F_1^2} \frac{Qa^2}{\kappa \text{Pr}(t_e - t_w)} \sum_{n=1}^{\infty} B_n V_0 \left(\gamma_n \frac{r}{r_1} \right) e^{-\lambda_n^2 x'} \quad (54)$$

where $V_0 \left(\gamma_n \frac{r}{r_1} \right) \equiv V_{0,n}$ and λ_n^2 are the eigenfunctions and eigenvalues of the new Sturm-Liouville problem:

$$\frac{d^2 V_{0,n}}{dr^2} + \frac{1}{r} \frac{dV_{0,n}}{dr} + \frac{4\lambda_n^2}{F_1^2} V_{0,n} = 0 \quad (55a)$$

$$\frac{dV_{0,n}}{dr} = 0 \text{ at } r = r_0; V_{0,n} = 0 \text{ at } r = r_1 \quad (55b)$$

and where $\gamma_n = (2r_1/F_1)\lambda_n$. The solution of equation (55a) that satisfies equation (55b) is

$$V_0 \left(\gamma_n \frac{r}{r_1} \right) \equiv V_{0,n} = -Y_1(k\gamma_n) J_0 \left(\gamma_n \frac{r}{r_1} \right) + J_1(k\gamma_n) Y_0 \left(\gamma_n \frac{r}{r_1} \right) \quad (56)$$

where the eigenvalues γ_n are obtained as the positive roots of

$$J_1(k\gamma_n) Y_0(\gamma_n) - Y_1(k\gamma_n) J_0(\gamma_n) = 0 \quad (57)$$

Values of the roots γ_n are given in reference 19 for several values of k less than unity. Values of k less than unity are physically inadmissible, however, as explained earlier.

TABLE III. - LISTING OF EIGENVALUES λ_n^2

Diffusivity parameter, k	Eigenvalue				
	λ_1^2	λ_2^2	λ_3^2	λ_4^2	λ_5^2
1.00	2.468	22.20	61.69	121.0	200.0
1.25	2.851	27.84	77.80	152.7	252.7
1.67	3.555	38.77	108.8	214.1	354.6
2.50	5.170	65.54	186.5	367.8	609.6
5.00	11.48	186.8	541.4	1066	1784

It was necessary, therefore, in the present investigation to calculate the eigenvalues of equation (57) for the values of k cited previously.

The first five eigenvalues $\lambda_n^2 = \lambda_n^2 / F_0 = \gamma_n^2 (k^2 - 1)^2 / 4$ are listed in table III for values of k of 1.00, 1.25, 1.67, 2.50, and 5.00. The eigenvalues λ_n^2 for k = 1.00 are given in reference 1 as

$$\lambda_n^2 (k=1) = \left(\frac{2n-1}{2} \pi \right)^2 ; n=1, 2, \dots \quad (58)$$

The next step in the analysis is to determine the coefficients B_n of equation (54). Applying the boundary condition at the channel entrance as given by equation (53c) results in

$$\sum_{n=1}^{\infty} B_n V_0 \left(\gamma_n \frac{r}{r_1} \right) = -g(r) \quad (59a)$$

According to Sturm-Liouville theory the coefficients B_n are then given by

$$B_n = - \frac{\int_{r_0}^{r_1} r g(r) V_0 \left(\gamma_n \frac{r}{r_1} \right) dr}{\int_{r_0}^{r_1} r V_0^2 \left(\gamma_n \frac{r}{r_1} \right) dr} \quad (59b)$$

The analytical evaluation of the coefficients B_n is carried out in appendix C. The coefficients B_n are obtained from

$$B_n = \frac{4r_1}{\gamma_n^2} \left[\frac{\left(\frac{dV_{0,n}}{dr} \right)_{r=r_1}}{\left(\frac{dV_{0,n}}{dr} \right)_{r=r_1}^2 - \left(\frac{k\gamma_n}{r_1} \right)^2 (V_{0,n})_{r=r_0}^2} \right]$$

$$= \frac{4r_1}{\gamma_n^2} \psi_n \quad (59c)$$

It will be useful in the subsequent analysis to define a quantity φ_n , given by

$$\varphi_n \equiv \frac{V_1^2(\gamma_n)}{V_1^2(\gamma_n) - k^2 V_0^2(k\gamma_n)} = -\frac{\gamma_n}{r_1} V_1(\gamma_n) \psi_n \quad (60)$$

where

$$V_0(k\gamma_n) = J_1(k\gamma_n)Y_0(k\gamma_n) - Y_1(k\gamma_n)J_0(k\gamma_n) \quad (61a)$$

and

$$V_1(\gamma_n) = -\frac{r_1}{\gamma_n} \left(\frac{dV_{0,n}}{dr} \right)_{r=r_1} = J_1(k\gamma_n)Y_1(\gamma_n) - Y_1(k\gamma_n)J_1(\gamma_n) \quad (61b)$$

In addition, it is convenient to define a new coefficient \bar{B}_n as

$$\bar{B}_n \equiv -\frac{B_n}{r_1(k^2 - 1)} \left(\frac{dV_0}{dr} \right)_{r=r_1}$$

$$= -\frac{4\varphi_n}{(k^2 - 1)\gamma_n^2} = -\frac{(k^2 - 1)\varphi_n}{\lambda_n^2} \quad (62)$$

TABLE IV. - VALUES OF COEFFICIENTS \bar{B}_n

Diffusivity parameter, k	Coefficient				
	\bar{B}_1	\bar{B}_2	\bar{B}_3	\bar{B}_4	\bar{B}_5
1.00	0.81000	0.09020	0.03242	0.01653	0.01000
1.25	.82994	.08125	.02898	.01475	.00891
1.67	.85528	.06991	.02462	.01249	.00753
2.50	.88744	.05502	.01899	.00957	.00576
5.00	.90314	.03507	.01150	.00570	.00341

Numerical values of \bar{B}_n are listed in table IV as a function of values of the parameter k. The values of \bar{B}_n for k = 1 are obtained from reference 1 as

$$\bar{B}_n = \frac{2}{\lambda_n^2} \quad (k = 1) \quad (63)$$

Complete solution. - Now that $T_{Q,d}$ and T_Q^* are known, they can be superposed as in equation (52) to obtain the solution that applies over the entire length of the channel. This is

$$\frac{T_Q}{Qa^2/\kappa(t_e - t_w)} = \frac{2}{F_1(k^2 - 1)} \left[r_0^2 \ln\left(\frac{r}{r_1}\right) - \frac{r^2 - r_1^2}{2} + \sum_{n=1}^{\infty} B_n V_0 \left(\gamma_n \frac{r}{r_1} \right) e^{-\lambda_n^2 x^+} \right] \quad (64)$$

In order to determine, in the later analysis, the local heat-transfer coefficients and Nusselt numbers, it is necessary to know the fluid mixed-mean temperature $t_{Q,b}$, which may be found as follows:

$$\begin{aligned} T_{Q,b} &\equiv \frac{t_{Q,b}}{t_e - t_w} = \frac{\int_{r_0}^{r_1} u T_Q r \, dr}{\int_{r_0}^{r_1} u r \, dr} \\ &= \frac{2}{r_1^2 - r_0^2} \int_{r_0}^{r_1} T_Q r \, dr \end{aligned} \quad (65)$$

since $u = U = \text{constant}$. The temperature distribution from equation (64) is introduced, and after integration and rearrangement there results

$$\frac{T_{Q,b}}{Qa^2/\kappa(t_e - t_w)} = \frac{4k^4 \ln k - (k^4 - 1) - 2(k^2 - 1)^2}{2(k^2 - 1)^3} - \sum_{n=1}^{\infty} \frac{\bar{B}_n}{\lambda_n^2} e^{-\lambda_n^2 x^+} \quad (66)$$

The situation of a liquid metal containing no heat sources and flowing in a channel with uniform wall temperatures is considered next. This problem is considered in references 2 and 3, but is repeated here for the sake of completeness.

Uniform Wall Temperature Without Internal Heat Generation

Fully developed solution. - The temperature $T_T(x', r)$ is the solution to equations (49). For large downstream distances, $T_{T,d}$ approaches zero; that is, $t_{T,d} \rightarrow t_w$. Therefore $T_T(x', r)$ can be obtained from the entrance region solution $T_T^*(x', r)$ defined by $T_T^* \equiv T_T - T_{T,d}$.

Entrance region solution. - The function $T_T^*(x', r)$ satisfies the equation

$$\frac{\partial T_T^*}{\partial x'} = \frac{F_1^2}{4} \frac{1}{r} \frac{\partial}{\partial r} \left(r \frac{\partial T_T^*}{\partial r} \right) \quad (67a)$$

with the boundary conditions

$$\left. \begin{aligned} \frac{\partial T_T^*}{\partial r} &= 0 \text{ at } r = r_0 \\ T_T^* &= 0 \text{ at } r = r_1 \end{aligned} \right\} \quad (67b)$$

At the channel entrance, the condition is

$$T_T^*(0, r) = 1 \quad (67c)$$

The solution to equation (67a) that also satisfies equation (67b) can be written

$$T_T^*(x', r) = \sum_{n=1}^{\infty} C_n V_0 \left(\gamma_n \frac{r}{r_1} \right) e^{-\lambda_n^2 x^+} \quad (68)$$

where $\gamma_n = (2r_1/F_1)\bar{\lambda}_n$ and $V_0(\gamma_n r/r_1)$ are the same eigenvalues and eigenfunctions obtained previously from equation (55). The new coefficients C_n are found by applying the boundary condition at $x' = 0$ (eq. (67c)) and using the properties of the Sturm-Liouville system with the result

$$C_n = \frac{\int_{r_0}^{r_1} V_0\left(\gamma_n \frac{r}{r_1}\right) r \, dr}{\int_{r_0}^{r_1} V_0^2\left(\gamma_n \frac{r}{r_1}\right) r \, dr} \quad (69a)$$

The integral in the numerator can be evaluated by substituting equation (55) for $V_0\left(\gamma_n \frac{r}{r_1}\right)$ and then integrating. The result of this operation is

$$\int_{r_0}^{r_1} V_0\left(\gamma_n \frac{r}{r_1}\right) r \, dr = -\frac{F_1^2 r_1}{4\bar{\lambda}_n^2} \left(\frac{dV_{0,n}}{dr} \right)_{r=r_1}$$

Hence, when the result from appendix C is used for the integral appearing in the denominator of equation (69a), the coefficients C_n are given by

$$C_n = -\frac{2}{r_1} \psi_n$$

New expansion coefficients \bar{C}_n are introduced for convenience and defined as

$$\bar{C}_n \equiv -\frac{F_1}{2} \frac{C_n}{r_1} \left(\frac{dV_{0,n}}{dr} \right)_{r=r_1} = (k^2 - 1)\varphi_n \quad (70)$$

TABLE V. - VALUES OF COEFFICIENTS \bar{C}_n

Diffusivity parameter, k	Coefficient				
	$-\bar{C}_1$	$-\bar{C}_2$	$-\bar{C}_3$	$-\bar{C}_4$	$-\bar{C}_5$
1.00	2.0000	2.0000	2.0000	2.0000	2.0000
1.25	2.3661	2.2617	2.2542	2.2521	2.2513
1.67	3.0382	2.7021	2.6796	2.6730	2.6708
2.50	4.5870	3.6058	3.5388	3.5199	3.5120
5.00	10.686	6.5522	6.2278	6.1241	6.0778

For $k = 1$ the coefficients \bar{C}_n are given in reference 1 as

$$\bar{C}_n = -2 \quad (k = 1) \quad (71)$$

Values of \bar{C}_n are listed in table V for

several values of the parameter k .

The mixed-mean temperature $t_{T,b}$ of the fluid is given by its definition

$$\begin{aligned} \frac{t_{T,b} - t_w}{t_e - t_w} &\equiv T_{T,b} = \frac{\int_{r_0}^{r_1} U T_T r dr}{\int_{r_0}^{r_1} U r dr} \\ &= \frac{2}{r_1^2 - r_0^2} \int_{r_0}^{r_1} T_T r dr \end{aligned} \quad (72)$$

Introducing equation (68) for $T_T(x', r)$ into equation (72) and carrying out the integration yields

$$T_{T,b} = - \sum_{n=1}^{\infty} \frac{\bar{C}_n}{\lambda_n^2} e^{-\lambda_n^2 x^+} \quad (73)$$

Combined Internal Heat Sources and Uniform Wall Temperature

The complete solution for the temperature $t(x^+, r)$ that applies for a heat-generating liquid metal flowing in a channel with uniform wall temperatures t_w is found by combining the solutions for T_Q and T_T in accordance with equation (47b) to obtain the result

$$\begin{aligned} \frac{t(x^+, r) - t_w}{t_e - t_w} = T(x^+, r) &= \frac{Qa^2}{\kappa(t_e - t_w)} \left\{ \frac{2}{F_1(k^2 - 1)} \left[r_0^2 \ln\left(\frac{r}{r_1}\right) - \frac{r^2 - r_1^2}{2} \right. \right. \\ &\quad \left. \left. + \sum_{n=1}^{\infty} B_n V_0 \left(\gamma_n \frac{r}{r_1} \right) e^{-\lambda_n^2 x^+} \right] \right\} + \sum_{n=1}^{\infty} C_n V_0 \left(\gamma_n \frac{r}{r_1} \right) e^{-\lambda_n^2 x^+} \end{aligned} \quad (74)$$

When the channel wall temperatures are specified, the longitudinal variation of the wall heat flux required to maintain the wall temperatures constant is of practical interest.

The heat-transfer rate q at the channel wall according to Fourier's law is given by

$$q = -\kappa \left(\frac{\partial t}{\partial y} \right)_{y=a}$$

$$= \frac{F_1}{2} \frac{\kappa(t_e - t_w)}{a} \left(\frac{1}{r} \frac{\partial T}{\partial r} \right)_{r=r_1} \quad (75)$$

The heat-transfer rate can be found by differentiating the temperature distribution given by equation (74) and evaluating the result at $r = r_1$ in accordance with equation (75) with the result

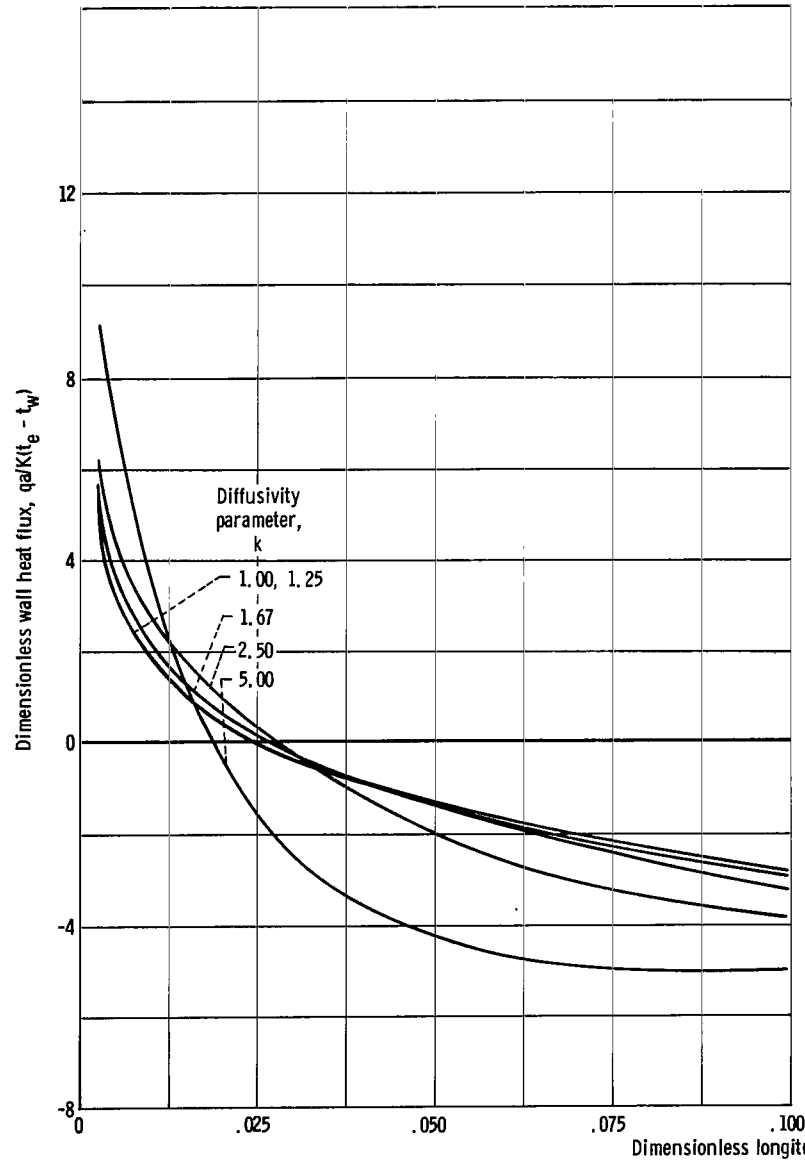
$$\frac{qa}{\kappa(t_e - t_w)} = N \left(1 - \sum_{n=1}^{\infty} \bar{B}_n e^{-\lambda_n^2 x^+} \right) - \sum_{n=1}^{\infty} \bar{C}_n e^{-\lambda_n^2 x^+} \quad (76)$$

where $N \equiv Qa^2/\kappa(t_e - t_w)$.

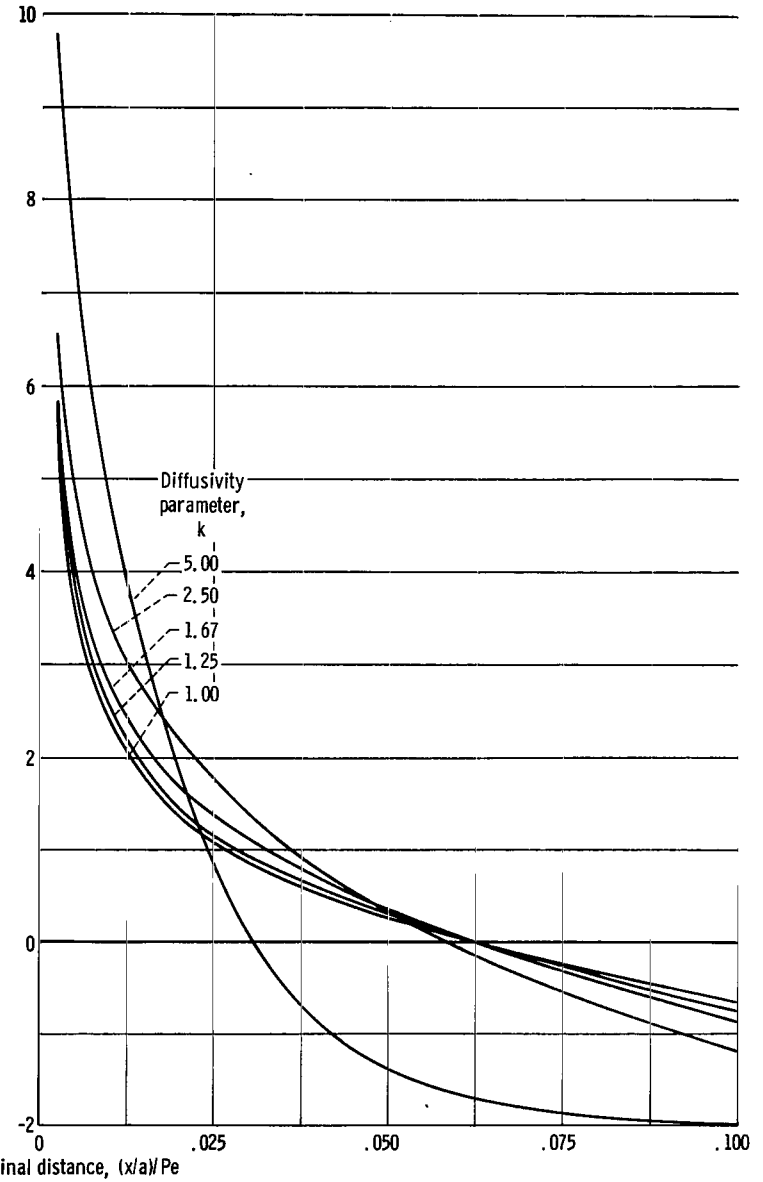
The parameter N indicates the importance of internal heat generation Q relative to that of temperature driving force $t_e - t_w$. In the present analysis Q is taken to be positive, but clearly $t_e - t_w$ may be either positive or negative. The parameter N , therefore, may also be either positive or negative. In view of this, illustrative heat-transfer results have been evaluated from equation (76) for values of N ranging from -5 to +5 and for several parametric values of k . This information is given in figure 7 as a function of the longitudinal position coordinate. It is worth additional emphasis that both the position coordinate and the parameter k contain the product of Reynolds and Prandtl numbers. It can be seen from figure 7 that, for negative values of N , the value of the wall heat flux q may change sign at some position along the channel length, which indicates a change in direction of the heat transfer at that location along the wall. It is noted, in addition, that, for all values of k , the local heat transfer approaches an asymptote that is dependent solely on the magnitude of N :

$$\left[\frac{qa}{\kappa(t_e - t_w)} \right]_d = N$$

This result is obtained from equation (76) by permitting x^+ to approach infinity therein. Thus, for $N = 0$ (no internal heat sources) the heat flux decreases to zero at large downstream distances.

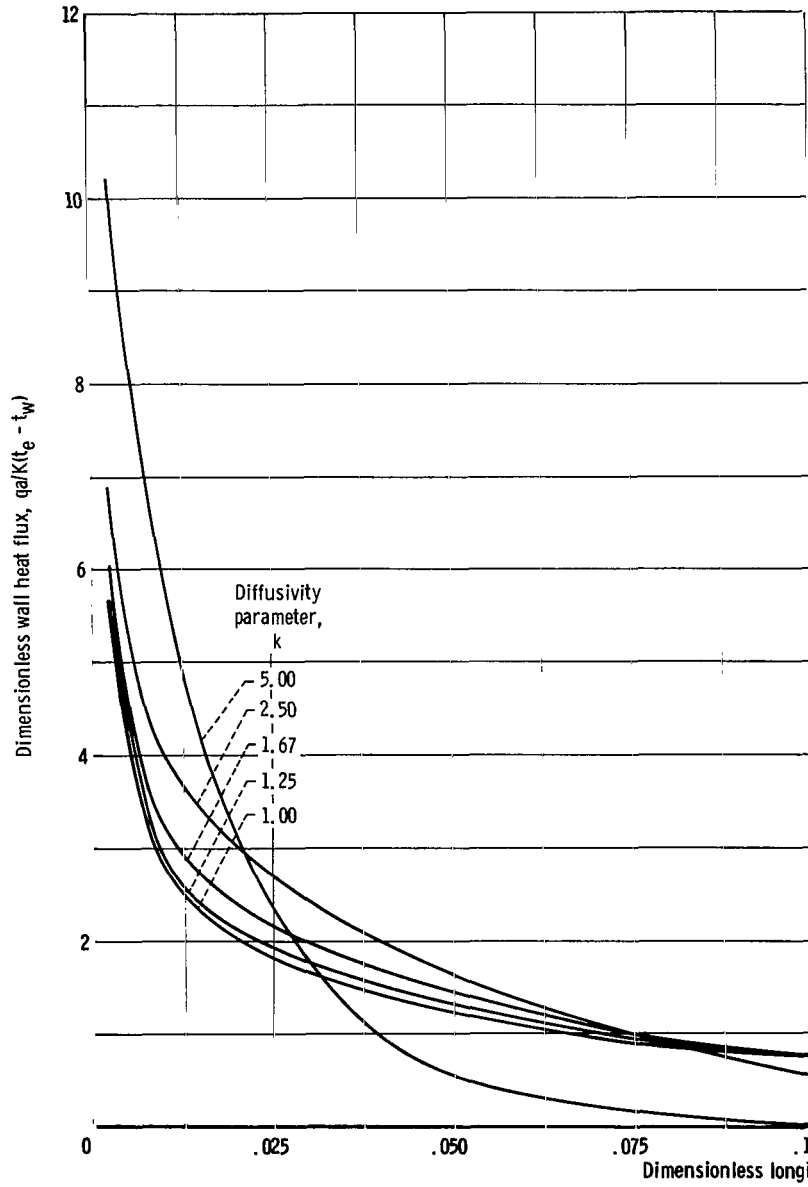


(a) Temperature driving force parameter, -5.

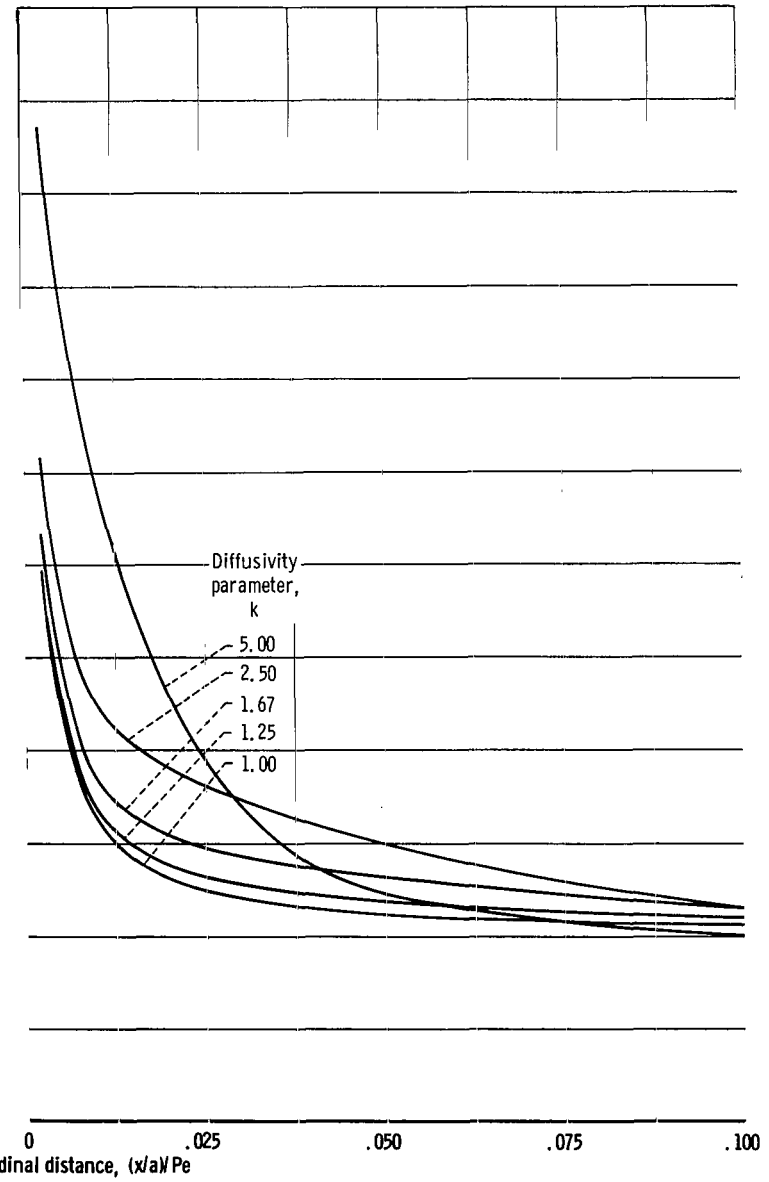


(b) Temperature driving force parameter, -2.

Figure 7. - Local heat flux results for internal heat generation with prescribed wall temperature.

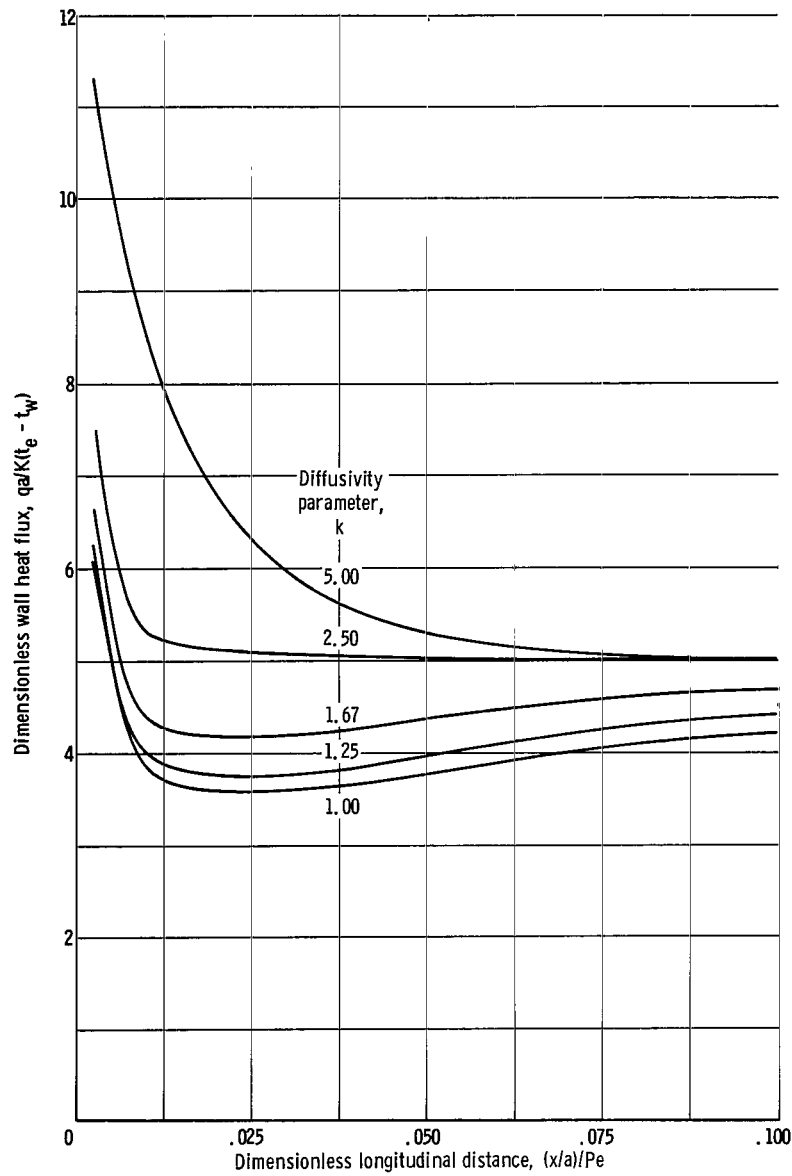


(c) Temperature driving force parameter, 0.



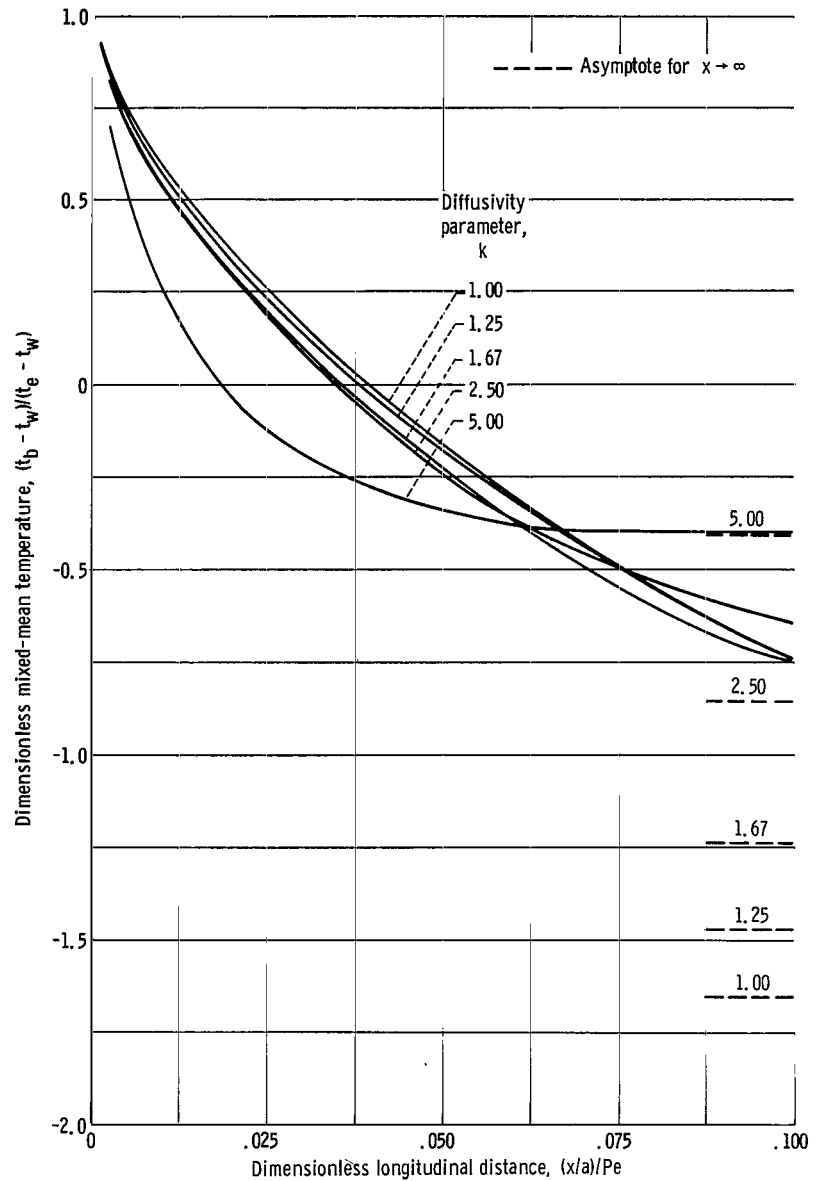
(d) Temperature driving force parameter, 2.

Figure 7. - Continued.



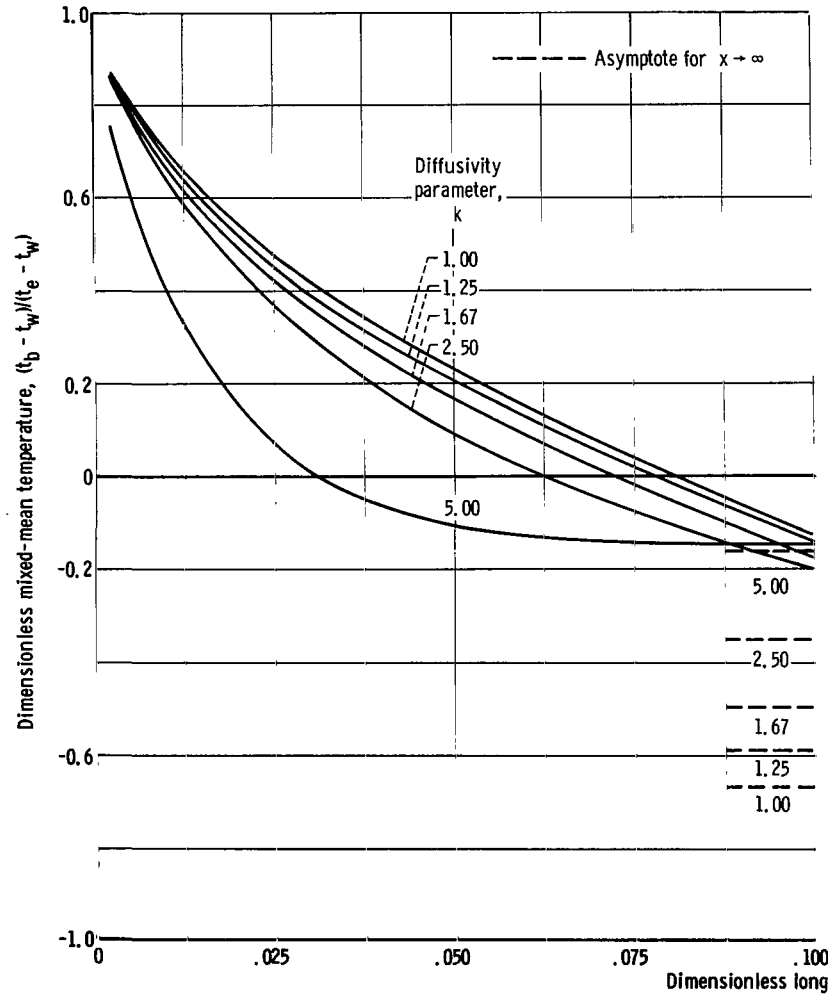
(e) Temperature driving force parameter, 5.

Figure 7. - Concluded.

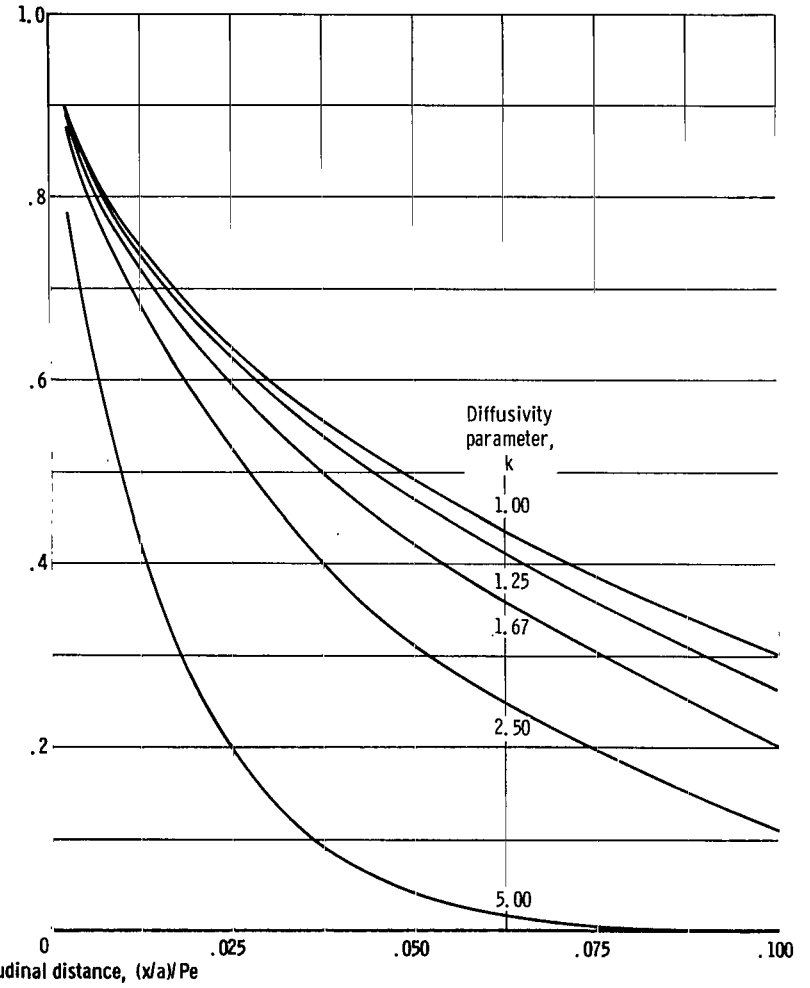


(a) Temperature driving force parameter, -5.

Figure 8. - Mixed-mean temperature results for internal heat generation with prescribed wall temperature.

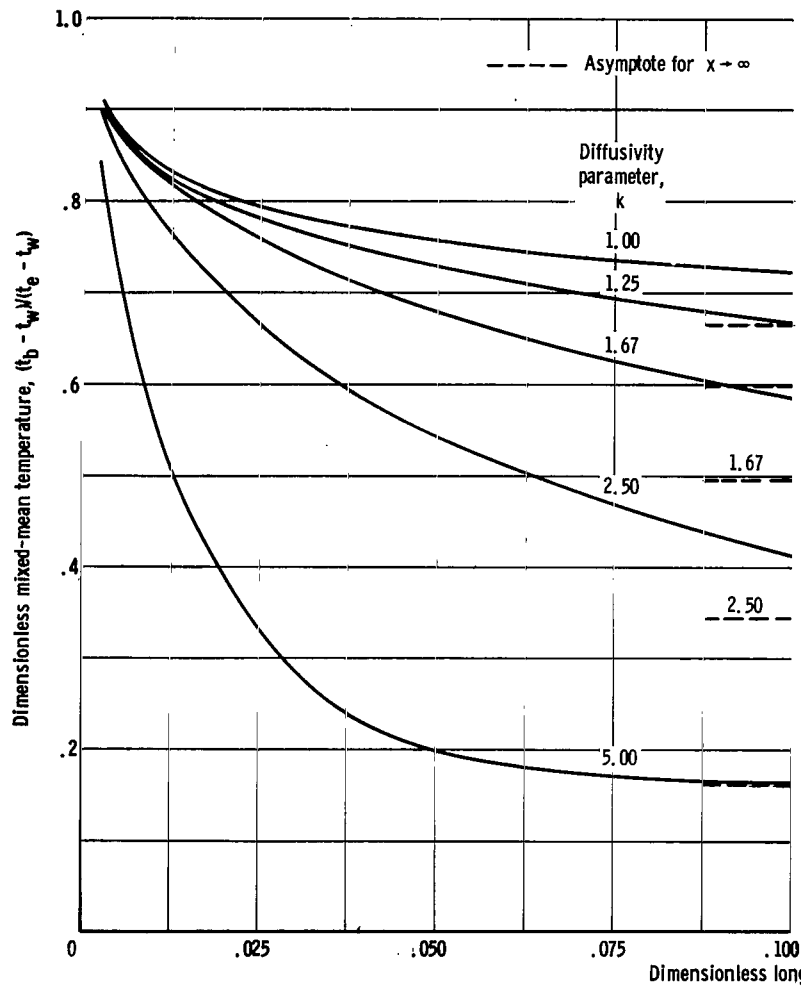


(b) Temperature driving force parameter, -2.

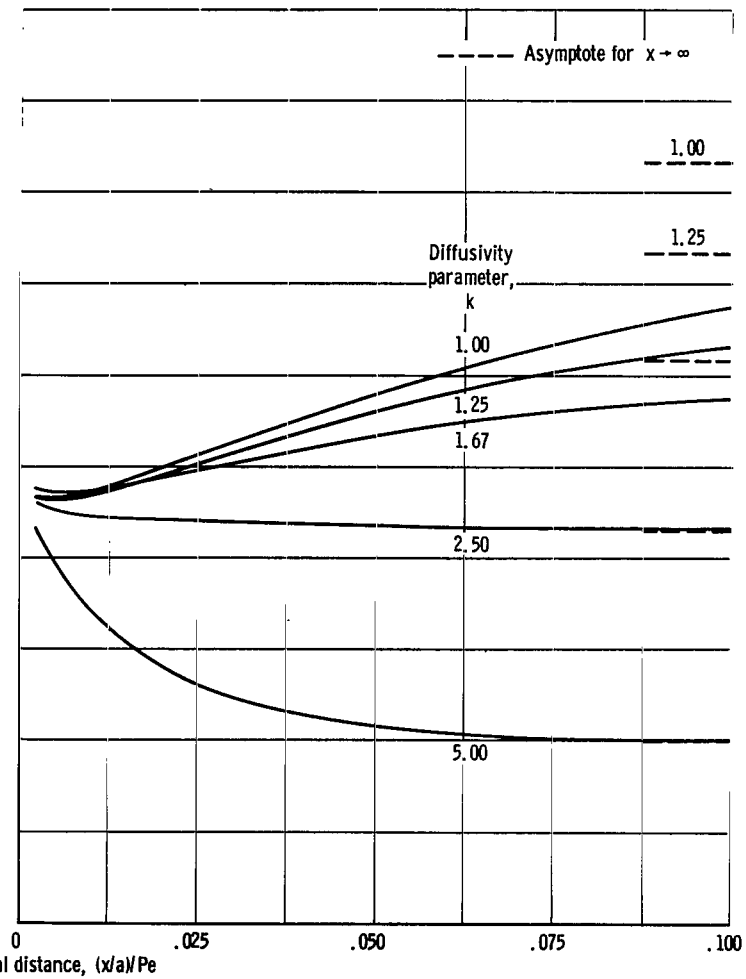


(c) Temperature driving force parameter, 0.

Figure 8. - Continued.



(d) Temperature driving force parameter, 2.



(e) Temperature driving force parameter, 5.

Figure 8. - Concluded.

The fluid mixed-mean temperature for the situation of combined internal heat generation and temperature driving force $t_e - t_w$ is computed from

$$\begin{aligned} \frac{t_b - t_w}{t_e - t_w} &\equiv T_b = T_{Q,b} + T_{T,b} \\ &= N \left(H(k) - \sum_{n=1}^{\infty} \frac{\bar{B}_n}{\lambda_n^2} e^{-\lambda_n^2 x^+} \right) - \sum_{n=1}^{\infty} \frac{\bar{C}_n}{\lambda_n^2} e^{-\lambda_n^2 x^+} \end{aligned} \quad (77)$$

where

$$H(k) = \frac{4k^4 \ln k - (k^4 - 1) - 2(k^2 - 1)^2}{2(k^2 - 1)^3} \quad (78)$$

The similarity between equation (77) and the function $G(k)$, given by equation (40b), is noteworthy. Then for the fully developed situation ($x^+ \rightarrow \infty$),

$$T_{b,d} = \left(\frac{t_b - t_w}{t_e - t_w} \right)_d = NH(k) \quad (79)$$

Local dimensionless mixed-mean temperatures T_b have been evaluated from equation (77) and are plotted in figure 8. Also shown are the asymptotic values $T_{b,d}$ as given by equation (79). The curves of $(t_b - t_w)/(t_e - t_w)$ change continuously from an initial value of unity to an asymptote of $NH(k)$ as t_b varies from t_e to $t_w + N(t_e - t_w)H(k)$. In the absence of internal heat generation, the mixed-mean temperature asymptotically approaches the temperature of the walls.

A heat-transfer coefficient h and a Nusselt number Nu can now be determined from their respective definitions:

$$\begin{aligned} h &\equiv \frac{q}{t_b - t_w} \\ Nu &\equiv \frac{hD_H}{\kappa} = 4 \frac{qa}{\kappa(t_e - t_w)} \frac{t_e - t_w}{t_b - t_w} \end{aligned}$$

Substitution for $qa/\kappa(t_e - t_w)$ and $(t_e - t_w)/(t_b - t_w)$ from equations (76) and (77) leads to

$$\text{Nu} = 4 \frac{N \left(1 - \sum_{n=1}^{\infty} \bar{B}_n e^{-\lambda_n^2 x^+} \right) - \sum_{n=1}^{\infty} \bar{C}_n e^{-\lambda_n^2 x^+}}{N \left[H(k) - \sum_{n=1}^{\infty} \frac{\bar{B}_n}{\lambda_n^2} e^{-\lambda_n^2 x^+} \right] - \sum_{n=1}^{\infty} \frac{\bar{C}_n}{\lambda_n^2} e^{-\lambda_n^2 x^+}} \quad (80)$$

Before equation (80) is considered further, it is of interest to examine the fully developed heat-transfer conditions. For nonzero values of N , the fully developed condition is obtained from equation (80) when $x^+ \rightarrow \infty$ and the Nusselt number Nu_d is given by

$$\text{Nu}_d = \frac{4}{H(k)} \quad (81)$$

It is noteworthy that this result is independent of the parameter N . For molecular-conduction heat transfer, $k = 1$, $H(1) = 1/3$, and the fully developed Nusselt number is

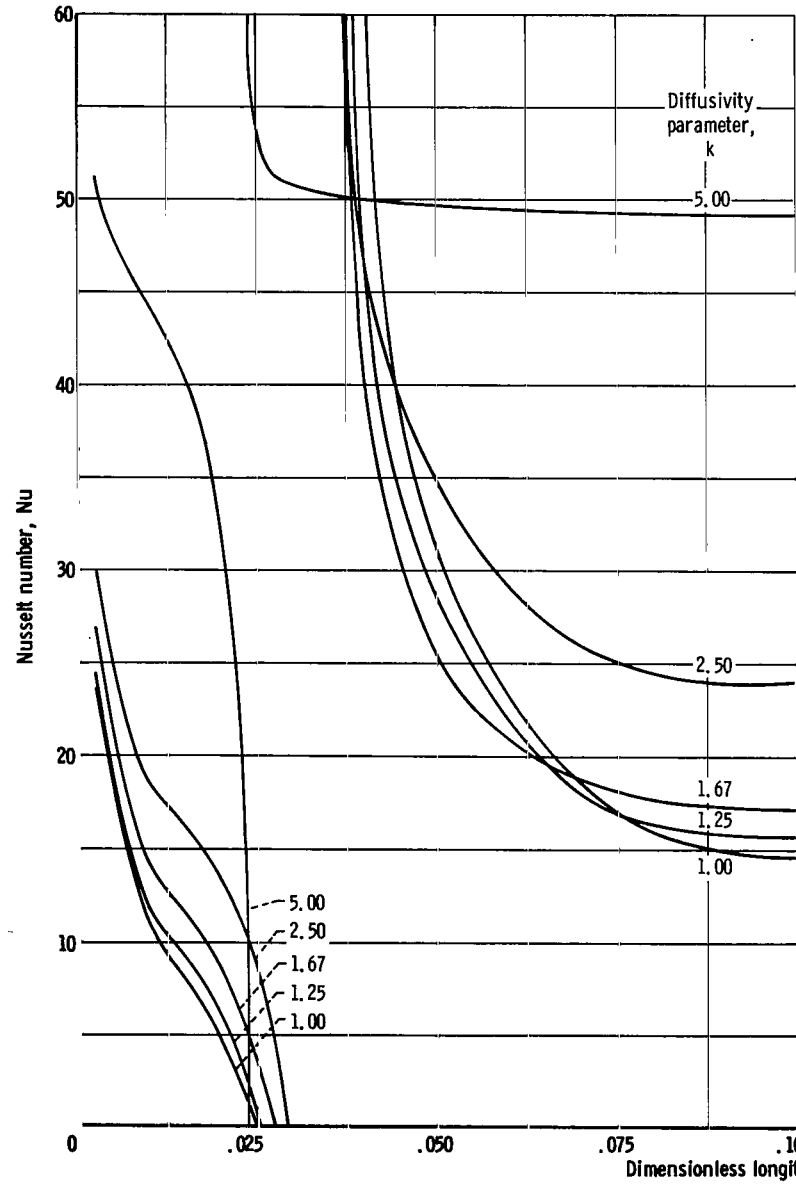
$$\text{Nu}_d = 12 \quad (k = 1) \quad (82)$$

which agrees with the result given in reference 1.

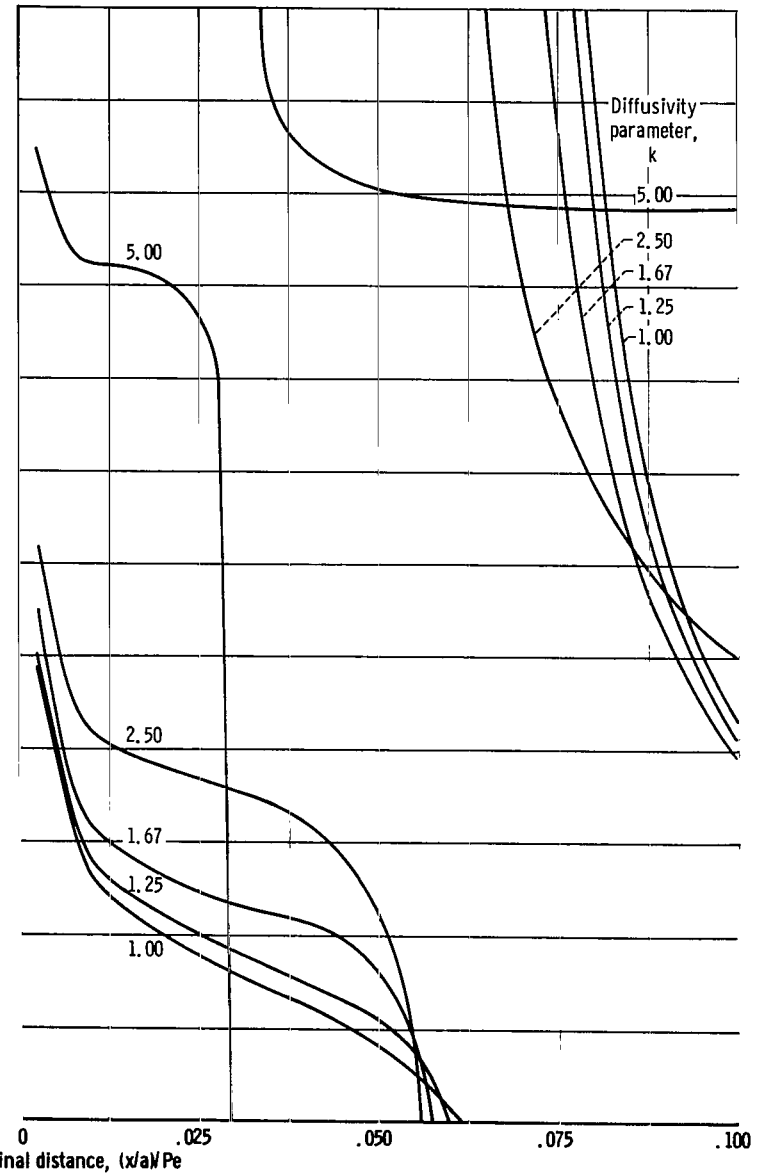
The Nusselt number at any axial location for $N = 0$ is obtained from equation (80) as the simpler expression

$$\text{Nu} = \frac{4 \sum_{n=1}^{\infty} \bar{C}_n e^{-\lambda_n^2 x^+}}{\sum_{n=1}^{\infty} \frac{\bar{C}_n}{\lambda_n^2} e^{-\lambda_n^2 x^+}} \quad (83)$$

The fully developed heat-transfer condition in the present situation occurs for x^+ sufficiently large so that only the first term of each of the series need be considered. The

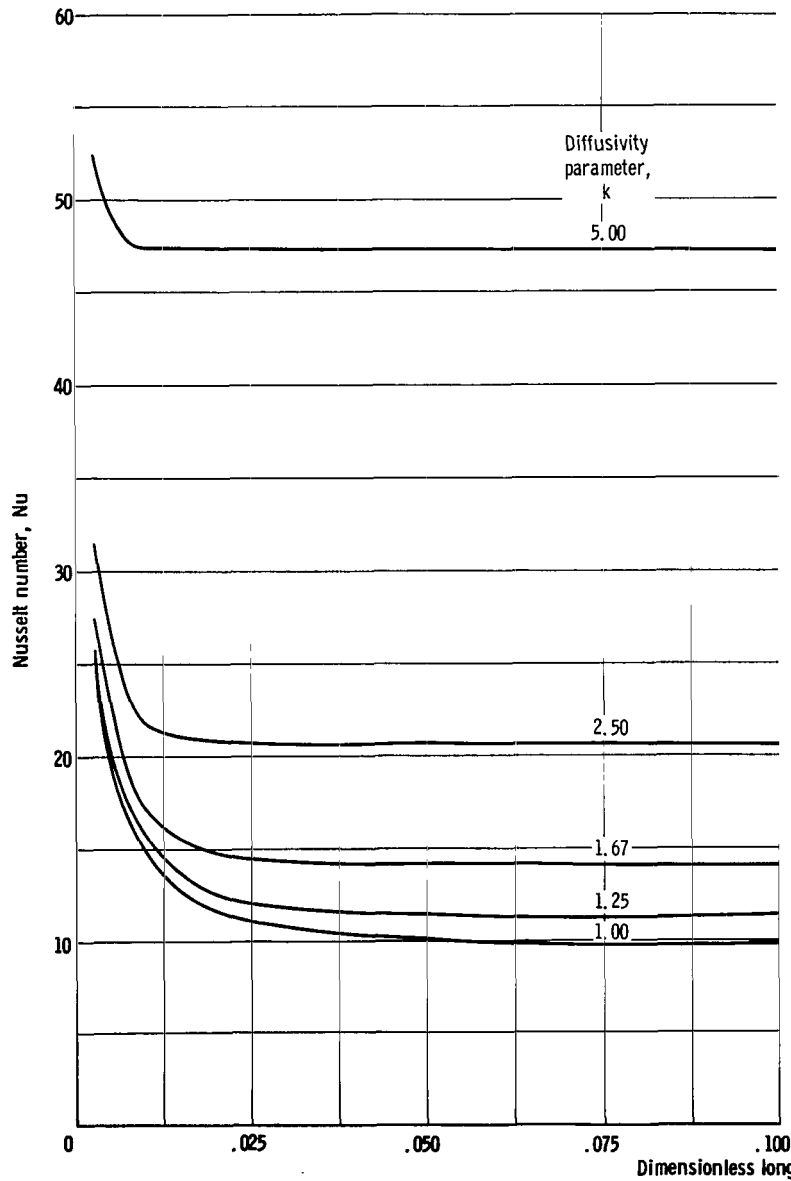


(a) Temperature driving force parameter, -5.

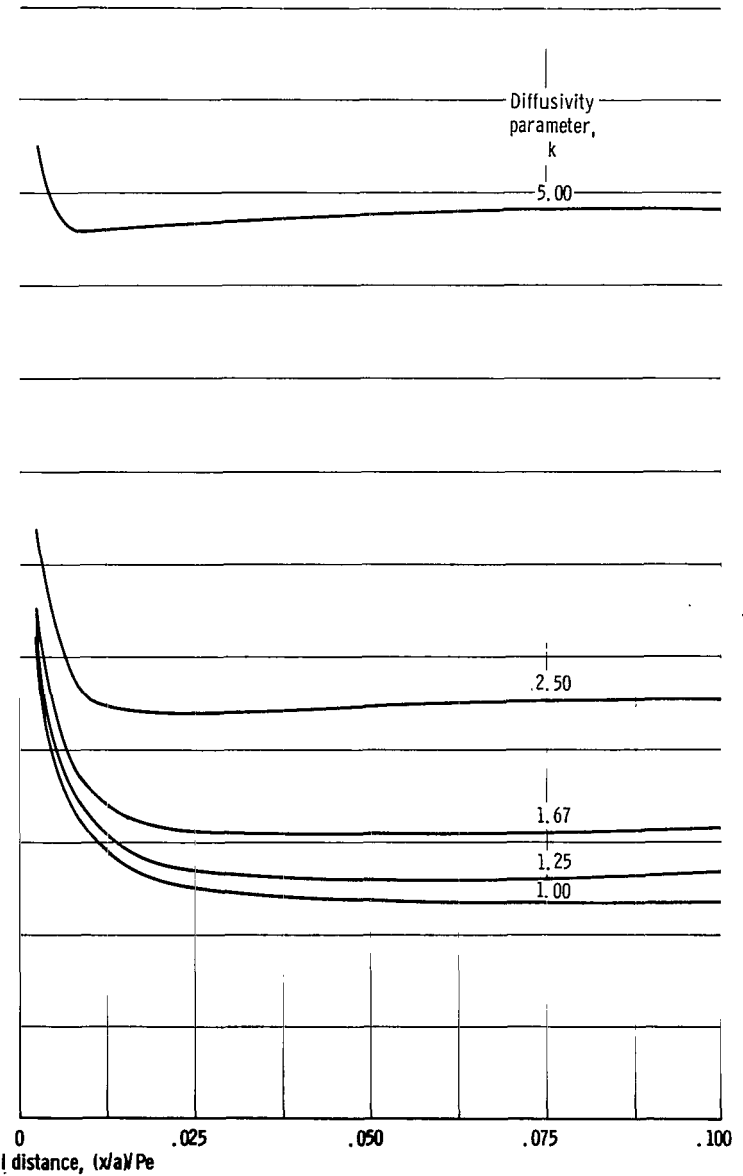


(b) Temperature driving force parameter, -2.

Figure 9. - Nusselt number results for internal heat generation with uniform wall temperature.



(c) Temperature driving force parameter, 0.



(d) Temperature driving force parameter, 2.

Figure 9. - Continued.

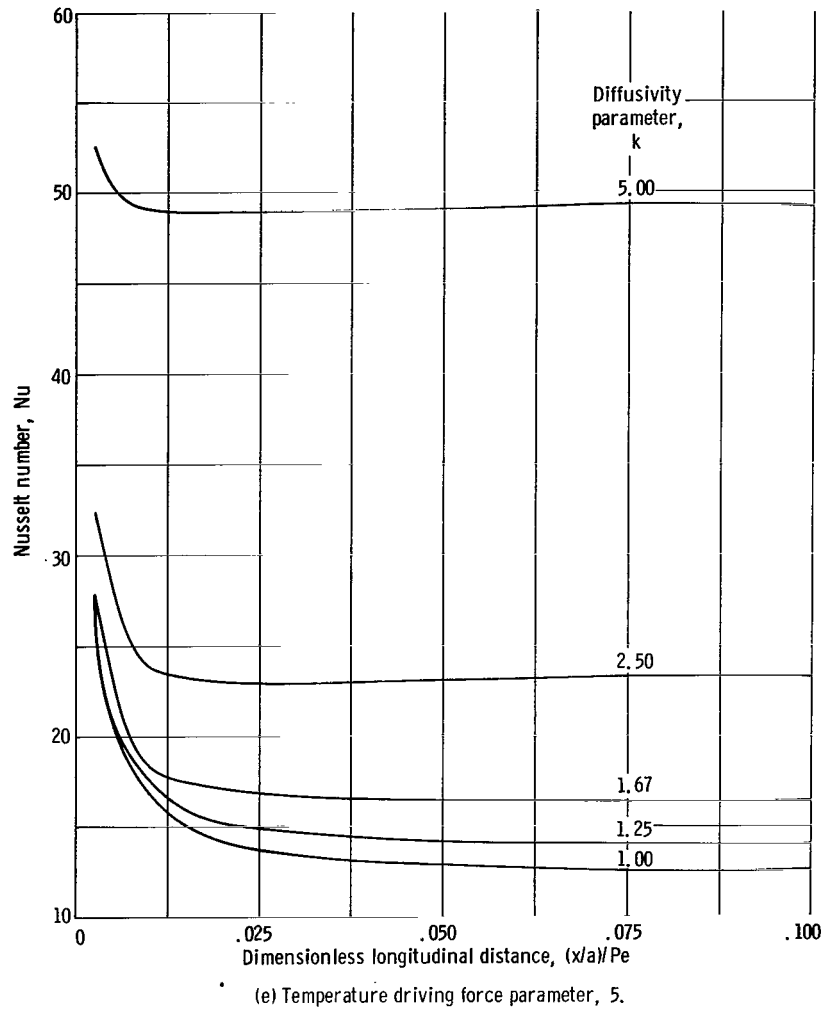


Figure 9. - Concluded.

fully developed Nusselt number then follows as the very simple expression

$$Nu_d = 4\lambda_1^2 \quad (84)$$

For $k = 1$ (molecular-conduction heat transfer),

$$\begin{aligned} Nu_d(k = 1) &= 4\left(\frac{\pi}{2}\right)^2 \\ &= 9.87 \end{aligned} \quad (85)$$

in agreement with the result given in reference 1.

Figure 9 shows the variation of the local Nusselt number as a function of the longi-

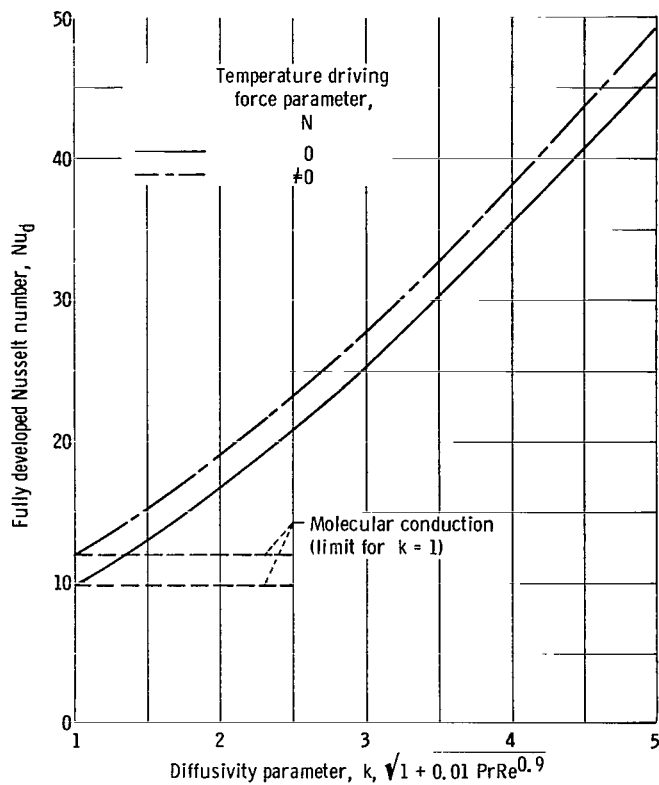


Figure 10. - Fully developed Nusselt number results for uniform wall temperature without internal heat sources and for uniform wall temperature with internal heat generation.

tudinal position coordinate for values of N ranging from -5 to $+5$, with k appearing as the family parameter. An overall inspection of the figure reveals that, for positive values of N (including the case where $N = 0$), the local Nusselt numbers are large near the channel entrance and decrease continuously with increasing downstream distance. The Nusselt numbers plotted in figure 9 for negative values of N , however, indicate that the definition of the heat-transfer coefficient can become meaningless in these instances. This is due to the fact that the mixed-mean fluid temperature can become zero, or can have a sign different from that of the wall heat flux. Thus, zeroes and infinities can exist in the Nusselt numbers.

Numerical values of the fully developed Nusselt number have been evaluated from equations (81) and (84) as a

function of the parameter k , and are plotted in figure 10. Inspection of the figure reveals that the effect of internal heat generation is to raise the Nusselt number above the value attained by a nongenerating liquid metal. It is interesting to compare figure 10 with its counterpart for uniform heat flux, figure 6 (p. 21). These figures portray similar trends and, in addition, the numerical values are not drastically different.

The fully established Nusselt number results, in the absence of internal heat sources (eq. (84)), have been compared to the values calculated by Martinelli for uniform wall heat flux and presented in the discussion section of reference 14. The tabulated Nusselt number values in the Prandtl number range of 0.001 to 0.100 , for Reynolds numbers from 10^4 to 10^6 , were considered here for comparison. The comparison (fig. 11) illustrates that the two sets of calculations are in fairly good agreement, with the uniform-wall-temperature Nusselt numbers falling about 10 percent below the uniform-wall-heat-flux Nusselt numbers.

Within the author's knowledge there are no uniform, symmetrical wall-temperature analyses for liquid metals flowing turbulently between parallel plates for comparison. Reference 15 considers heat transfer to a turbulently flowing fluid between parallel walls with asymmetric, uniform wall temperatures. It is concluded in reference 15 that, for

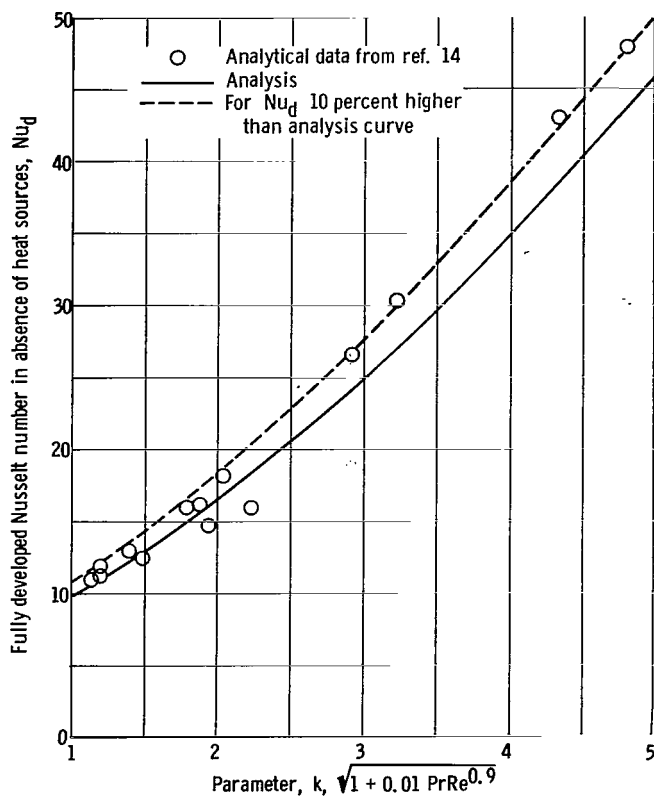


Figure 11. - Comparison of analysis for fully developed Nusselt number for uniform wall temperature without internal heat sources to numerical data obtained from reference 14.

the case of equal wall temperatures, the solution given therein can be shown to coincide with the solutions given in reference 12 for the case of equal wall temperatures. Reference 12, however, treats the situation of heat transfer to fluids flowing between parallel plates with uniform wall heat fluxes and the conclusion drawn is therefore not clear.

Presently available experimental data are not sufficiently extensive to establish the accuracy of the Nusselt numbers given by equations (84) and (85).

Within the author's knowledge there are also no heat-transfer analyses for heat-generating liquid metals flowing between parallel plates that apply over the entire length of the duct and that consider simultaneous transfer of heat by molecular conduction and eddy diffusion. There are, in addition, presently no experimental results for liquid metal flow

between parallel plates with internal heat generation with which to compare the theoretical results.

CONCLUDING REMARKS

Solutions have been obtained for heat transfer to liquid metals flowing turbulently between parallel plates with heat sources in the fluid stream. In order to provide mathematical simplicity, the slug-flow model for the turbulent velocity distribution was utilized for the analyses. The effect of transverse eddy diffusivity variations, of importance for high Reynolds number systems, has been included through the use of an idealized eddy diffusivity function. This function approximates the actual one in the heat-transfer regions of importance.

The present analyses allow for consideration of Reynolds numbers ranging from 5×10^3 to approximately 10^6 , in virtue of consideration of transverse heat flow by turbulent eddying as well as by molecular conduction. Various quantities of engineering interest for both uniform wall heat flux and uniform wall temperature cases are determined in both

the thermal entrance and fully developed regions as functions of ratios of heat generation rate to wall heat transfer or temperature driving force, a dimensionless axial distance modulus, and a diffusivity parameter k . It has been shown that the effects of Reynolds and Prandtl numbers can be expressed concisely by the diffusivity parameter.

Evidence presented indicates that the fully developed Nusselt number solutions reduce correctly to known molecular-conduction heat-transfer results as k approaches unity. The present solutions, moreover, are shown by comparison to give satisfactory accuracy in the limiting case of no internal heat generation in the liquid metal. A truly quantitative comparison would require, on the theoretical side, inclusion of slightly more accurate velocity and eddy diffusivity descriptions in the boundary value problems and, on the experimental side, experimental data for the case in which there is internal heat generation in the flowing liquid metal.

The results indicate the effects of turbulent or eddy diffusivity and internal heat sources on the complicated problem of heat transfer to a flowing liquid metal, and it is believed that the simple engineering approach to the problem demonstrated here should be adequate for preliminary design purposes.

Lewis Research Center,
National Aeronautics and Space Administration,
Cleveland, Ohio, July 20, 1966,
129-01-09-07-22.

APPENDIX A

SYMBOLS

A_m	coefficients in series expansion of temperature for case of wall heat transfer and no internal heat sources, $\frac{a_m}{J_1(kW_m)}$	F_1	function of average value of ψ and of Reynolds modulus, $0.01 \bar{\psi} Re^{0.9}$
\bar{A}_m	coefficients defined by product $A_m V_0(w_m)$	$G(r)$	transverse temperature distribution in fully developed region for case of wall heat transfer and no internal heat generation
a	half-height of channel	$G(k)$	function of k given by eq. (40b)
a_m	coefficients in series expansion of temperature for case of wall heat transfer and no internal heat generation	$g(r)$	function of r defined by eq. (53c)
B_n	coefficients in series expansion of temperature for case of internal heat sources and zero wall temperature	$H(k)$	function of k defined by eq. (78)
\bar{B}_n	coefficient defined by eq. (62)	h	local heat-transfer coefficient, $q/(t_w - t_b)$ or $q_w/(t_w - t_b)$
C_n	coefficient in series expansion of temperature for case of uniform wall temperature and no internal heat generation	I_1	integral defined by eq. (B7)
\bar{C}_n	coefficient defined by eq. (70)	I_2	integral defined by eq. (B12)
c_1	constant of integration	I_3	integral defined by eq. (C1)
c_2	constant of integration	I_4	integral defined by eq. (C6)
c_p	specific heat of fluid at constant pressure	J_0	zero order Bessel functions of first kind
D_H	hydraulic diameter of duct, $4a$	J_1	first order Bessel functions of first kind
F_0	reciprocal of Prandtl modulus, $1/Pr$	k	diffusivity parameter, $r_0/r_1 = \sqrt{1 + 0.01 \bar{\psi} Pr Re^{0.9}}$
		N	ratio of internal heat generation rate to temperature driving force, $Qa^2/\kappa(t_e - t_w)$
		Nu	local Nusselt modulus, hD_H/κ
		Pe	Péclet number, $RePr$
		Pr	Prandtl number, ν/α

Q	heat generation rate/volume	Y_1	first order Bessel functions of second kind
q	local heat-transfer rate per unit area at channel wall	y	transverse coordinate measured from channel centerline
q_w	prescribed wall heat flux	y'	dimensionless transverse coordinate, y/a
R	ratio of heat generation rate to wall heat flux, Qa/q_w	α	molecular diffusivity for heat, $\kappa/\rho c_p$
Re	Reynolds number, $4aU/\nu$	$\bar{\beta}$	separation constant
r	transformed coordinate, $\sqrt{F_0 + F_1(1 - y')}$	$\bar{\beta}_m$	eigenvalues defined by $\bar{\beta}_m = (F_1/2r_1)w_m$
r_0	value of r at $y' = 0$, $\sqrt{F_0 + F_1}$	β_m^2	eigenvalues defined by $\beta_m^2 = \bar{\beta}_m^2/F_0$
r_1	value of r at $y' = 1$, $\sqrt{F_0}$	γ	separation constant
T	dimensionless temperature, $(t - t_w)/(t_e - t_w)$	γ_n	eigenvalues of eq. (57), $(2r_1/F_1)\bar{\lambda}_n$
t	fluid temperature	ϵ	eddy diffusivity
U	uniform velocity in x-direction	ϵ_H	eddy diffusivity of heat
u(y)	fluid velocity in x-direction	ϵ_M	eddy diffusivity of momentum
V_0	linear combination of zero order Bessel functions, eqs. (30) and (56)	θ	function of r, eq. (21)
$V_{0,n}$	linear combination of zero order Bessel functions, eq. (56)	κ	thermal conductivity
V_1	linear combination of first order Bessel functions, eq. (61b)	λ	eigenvalue
w_m	modified eigenvalue, $(2r_1/F_1)\bar{\beta}_m$	$\bar{\lambda}_n$	eigenvalues defined by $\bar{\lambda}_n = (F_1/2r_1)\gamma_n$
x	longitudinal coordinate measured from channel entrance	λ_n^2	eigenvalues defined by $\bar{\lambda}_n^2/F_0$
x'	dimensionless longitudinal coordinate, $4x/aRe$	ν	kinematic viscosity
x^+	dimensionless longitudinal coordinate, $x'/Pr = 4x/aPe$	ρ	fluid density
Y_0	zero order Bessel functions of second kind	τ	function of x, eq. (21)
		φ_n	function defined by eq. (60)
		ψ	ratio of eddy diffusivity for heat transfer to that for momentum transfer, ϵ_H/ϵ_M
		$\bar{\psi}$	average value of ψ

ψ_n function defined by eq. (59c)

Subscripts:

b bulk or mixed-mean condition

d developed

e entrance

Q internal heat generation, insulated
wall or zero wall temperature

q wall heat flux, no heat generation

T prescribed wall temperature, no
internal heat generation

w wall

Superscript:

* entrance region

APPENDIX B

EVALUATION OF SERIES COEFFICIENTS A_m

The coefficients A_m of the series expansion (eq. (28)) are determined as the quotient of two integrals (eq. (31b)):

$$A_m = - \frac{\int_{r_0}^{r_1} r G(r) V_0 \left(w_m \frac{r}{r_1} \right) dr}{\int_{r_0}^{r_1} r V_0^2 \left(w_m \frac{r}{r_1} \right) dr} \quad (31b)$$

In order to be able to solve for the coefficients A_m as the quotient of the two known integrals, it is necessary that the sequence of functions $V_0 \left(w_m \frac{r}{r_1} \right)$ form a system orthogonal with respect to the weight function r over the interval (r_0, r_1) . This means that the functions have the property

$$\int_{r_0}^{r_1} r V_0 \left(w_m \frac{r}{r_1} \right) V_0 \left(w_n \frac{r}{r_1} \right) dr = 0 \quad m \neq n \quad (B1)$$

The orthogonality of the set of characteristic functions $V_0 \left(w_m \frac{r}{r_1} \right)$ will now be demonstrated.

Let $V_0 \left(w_m \frac{r}{r_1} \right) \equiv V_{0,m}$ and $V_0 \left(w_n \frac{r}{r_1} \right) \equiv V_{0,n}$ be the solutions associated with two distinct values of β , namely, β_m and β_n . This means that

$$\frac{1}{r} \frac{d}{dr} \left(r \frac{dV_{0,m}}{dr} \right) + \frac{4\beta_m^2}{F_1^2} V_{0,m} = 0 \quad (B2)$$

with $dV_{0,m}/dr = 0$ at $r = r_0$ and $r = r_1$, and

$$\frac{1}{r} \frac{1}{dr} \left(r \frac{dV_{0,n}}{dr} \right) + \frac{\bar{\beta}_n^2}{F_1^2} V_{0,n} = 0 \quad (\text{B3})$$

with $dV_{0,n}/dr = 0$ at $r = r_0$ and $r = r_1$. Equation (B2) is multiplied by $V_{0,n}$ and equation (B3) by $V_{0,m}$, and then equation (B3) is subtracted from (B2). The result, after transposing, is

$$\frac{4}{F_1^2} (\bar{\beta}_m^2 - \bar{\beta}_n^2) r V_{0,m} V_{0,n} = -\frac{d}{dr} \left[r \left(V_{0,n} \frac{dV_{0,m}}{dr} - V_{0,m} \frac{dV_{0,n}}{dr} \right) \right]$$

If this equation is integrated between r_0 and r_1 , there is obtained the result

$$(\bar{\beta}_m^2 - \bar{\beta}_n^2) \int_{r_0}^{r_1} r V_{0,m} V_{0,n} dr = -\frac{F_1^2}{4} \left[r \left(V_{0,n} \frac{dV_{0,m}}{dr} - V_{0,m} \frac{dV_{0,n}}{dr} \right) \right]_{r_0}^{r_1} \quad (\text{B4})$$

The right side of equation (B4) is zero in virtue of the boundary conditions cited previously, and therefore

$$(\bar{\beta}_m^2 - \bar{\beta}_n^2) \int_{r_0}^{r_1} r V_{0,m} V_{0,n} dr = 0 \quad (\text{B5})$$

Since $\bar{\beta}_m$ and $\bar{\beta}_n$ are two distinct values of $\bar{\beta}$, the difference $\bar{\beta}_m^2 - \bar{\beta}_n^2$ cannot vanish. Hence

$$\int_{r_0}^{r_1} r V_0 \left(w_m \frac{r}{r_1} \right) V_0 \left(w_m \frac{r}{r_1} \right) dr = 0 \quad n \neq m \quad (\text{B6})$$

and orthogonality of the functions is demonstrated.

Consider again equation (31b). Let I_1 equal the integral appearing in the denominator:

$$I_1 = \int_{r_0}^{r_1} r V_0^2 \left(w_m \frac{r}{r_1} \right) dr \quad (\text{B7})$$

The functions $V_0 \left(w \frac{r}{r_1} \right)$ satisfy the differential Bessel equation

$$\frac{d}{dr} \left(r \frac{dV_0}{dr} \right) + \frac{4\beta^2}{F_1^2} r V_0 = 0 \quad (\text{B8})$$

If this equation is multiplied by $2r(dV_0/dr)$, and the resulting equation is integrated by parts over the range r_0 to r_1 , there results

$$\int_{r_0}^{r_1} r V_0^2 \left(w \frac{r}{r_1} \right) dr = \frac{\left[\left(r \frac{dV_0}{dr} \right)^2 + \frac{4\beta^2}{F_1^2} (r V_0)^2 \right]_{r_0}^{r_1}}{\frac{8\beta^2}{F_1^2}} \quad (\text{B9})$$

Into this expression there are substituted the boundary conditions

$$\frac{dV_0}{dr} = 0 \text{ at } r = r_0 \text{ and } r_1 \quad (\text{B10})$$

which give

$$\int_{r_0}^{r_1} r V_0^2 \left(w_m \frac{r}{r_1} \right) dr = \frac{1}{2} \left[r^2 V_0^2 \left(w_m \frac{r}{r_1} \right) \right]_{r_0}^{r_1}$$

and thus

$$I_1 = \frac{r_1^2}{2} \left[V_0^2(w_m) - k^2 V_0^2(kw_m) \right] \quad (B11)$$

Consider next the integral appearing in the numerator of equation (31b):

$$I_2 = \int_{r_0}^{r_1} r G(r) V_0 \left(w_m \frac{r}{r_1} \right) dr \quad (B12)$$

The integral I_2 can be evaluated by substituting $G(r)$ from equation (19), integrating by parts, and utilizing equations (B8) and (B10). This process gives finally

$$\begin{aligned} I_2 &= \frac{F_0}{2\beta_n^2} \left[(r^2 - r_0^2) V_0 \right]_{r_0}^{r_1} \\ &= \frac{2r_1^4 V_0(w_m)}{(r_1^2 - r_0^2) w_m^2} \end{aligned} \quad (B13)$$

Therefore, when equations (31b), (B11), and (B13) are used,

$$A_m = - \frac{4r_1^2 V_0(w_m)}{(r_1^2 - r_0^2) w_m^2 \left[V_0^2(w_m) - k^2 V_0^2(kw_m) \right]}$$

Substituting $k = r_0/r_1$ yields

$$A_m = \frac{4V_0(w_m)}{w_m^2 (k^2 - 1) \left[V_0^2(w_m) - k^2 V_0^2(kw_m) \right]} \quad (B14)$$

APPENDIX C

EVALUATION OF SERIES COEFFICIENTS B_n

The coefficients B_n of the series expansion (eq. (54)) are determined as the quotient of two integrals (eq. (59b)):

$$B_n = - \frac{\int_{r_0}^{r_1} r g(r) V_0 \left(\gamma_n \frac{r}{r_1} \right) dr}{\int_{r_0}^{r_1} r V_0^2 \left(\gamma_n \frac{r}{r_1} \right) dr} \quad (59b)$$

As was the case for the sequence of functions $V_0 \left(w_m \frac{r}{r_1} \right)$, the present functions $V_0 \left(\gamma_n \frac{r}{r_1} \right)$ form a system that is orthogonal with respect to the weight function r over the interval (r_0, r_1) . The proof follows the procedure given in appendix B and need not be repeated here. Hence, it is possible to solve for the B_n in the manner prescribed by equation (59b).

The general solution to the integral

$$I_3 = \int_{r_0}^{r_1} r V_0^2 \left(\gamma \frac{r}{r_1} \right) dr \quad (C1)$$

may be obtained by the technique used in solving the integral I_1 in appendix B. The result is

$$I_3 = \frac{\left[\left(r \frac{dV_0}{dr} \right)^2 + \frac{4F_0 \lambda^2}{F_1^2} (r V_0)^2 \right]_{r_0}^{r_1}}{\frac{8F_0 \lambda^2}{F_1^2}} \quad (C2)$$

Into this expression there are substituted the boundary conditions

$$\frac{dV_0}{dr} = 0 \text{ at } r = r_0; V_0 = 0 \text{ at } r = r_1 \quad (C3)$$

This substitution yields

$$I_3 = \frac{F_1^2}{8F_0\lambda^2} \left[r_1^2 \left(\frac{dV_0}{dr} \right)_{r=r_1}^2 - \frac{4F_0\lambda^2 r_0^2}{F_1^2} (V_0)_{r=r_0}^2 \right] \quad (C4)$$

and therefore

$$\begin{aligned} \int_{r_0}^{r_1} r V_0^2 \left(\gamma_n \frac{r}{r_1} \right) dr &= \frac{F_1^2 r_1^2}{8F_0\lambda_n^2} \left[\left(\frac{dV_{0,n}}{dr} \right)_{r=r_1}^2 - \frac{4F_0\lambda_n^2 r_0^2}{F_1^2 r_1^2} (V_{0,n})_{r=r_0}^2 \right] \\ &= \frac{F_1^2}{8\lambda_n^2} \left[\left(\frac{dV_{0,n}}{dr} \right)_{r=r_1}^2 - \left(\frac{k\gamma_n}{r_1} \right)^2 (V_{0,n})_{r=r_0}^2 \right] \end{aligned} \quad (C5)$$

It remains to investigate the integral I_4 , given by

$$I_4 = \int_{r_0}^{r_1} r g(r) V_0 \left(\gamma_n \frac{r}{r_1} \right) dr \quad (C6)$$

where $g(r) = r_0^2 \ln(r/r_1) - (1/2)(r^2 - r_1^2)$. The integral can be evaluated by substituting $g(r)$ from this expression and $V_0 \left(\gamma_n \frac{r}{r_1} \right)$ from equation (55a), namely,

$$V_0 \left(\gamma_n \frac{r}{r_1} \right) = - \frac{F_1^2}{4F_0\lambda_n^2} \left[\frac{1}{r} \frac{d}{dr} \left(r \frac{dV_{0,n}}{dr} \right) \right]$$

integrating by parts, and utilizing equation (55b). There is obtained the result

$$I_4 = -\frac{F_1^2}{4F_0\lambda_n^2} \left[r_1 g(r_1) \left(\frac{dV_{0,n}}{dr} \right)_{r=r_1} - r_0^2 (V_{0,n})_{r=r_0} + \frac{F_1^2 r_1}{2F_0\lambda_n^2} \left(\frac{dV_{0,n}}{dr} \right)_{r=r_1} + r_0^2 (V_{0,n})_{r=r_0} \right] \quad (C7)$$

Since $g(r_1) = 0$, however, equation (C7) may be rewritten in the simpler form

$$\begin{aligned} I_4 &= -\frac{F_1^4 r_1}{8F_0^2 \lambda_n^4} \left(\frac{dV_{0,n}}{dr} \right)_{r=r_1} \\ &= -\frac{F_1^4}{8F_0 r_1 \lambda_n^4} \left(\frac{dV_{0,n}}{dr} \right)_{r=r_1} \end{aligned} \quad (C8)$$

Therefore, using equations (59b), (C5), and (C8) yields

$$B_n = \frac{4r_1}{\gamma_n^2} \left[\frac{\left(\frac{dV_{0,n}}{dr} \right)_{r=r_1}}{\left(\frac{dV_0}{dr} \right)_{r=r_1}^2 - \left(\frac{k\gamma_n}{r_1} \right)^2 (V_{0,n})_{r=r_0}^2} \right] \quad (C9)$$

REFERENCES

1. Inman, Robert M. : Heat Transfer to Liquid-Metal Flow in a Round Tube or Flat Duct With Heat Sources in the Fluid Stream. NASA TN D-3473, 1966.
2. Poppendiek, H. F. : Heat Transfer in a Liquid Metal Flowing Turbulently Through a Channel With a Step Function Boundary Temperature. NASA Memo 2-5-59W, 1959.
3. Poppendiek, H. F. : Turbulent Liquid-Metal Heat Transfer in Channels. Nucl. Sci. Engr., vol. 5, no. 6, June 1959, pp. 390-404.
4. Brown, H. E. ; Amstead, B. H. ; and Short, B. E. : Temperature and Velocity Distribution and Transfer of Heat in a Liquid Metal. ASME Trans., vol. 79, no. 2, Feb. 1957, pp. 279-285.
5. Azer, N. Z. ; and Chao, B. T. : A Mechanism of Turbulent Heat Transfer in Liquid Metals. Int. Heat Mass Trans., vol. 1, 1960, pp. 121-138.
6. Azer, N. Z. ; and Chao, B. T. : Turbulent Heat Transfer in Liquid Metals - Fully Developed Pipe Flow with Constant Wall Temperature. Int. Heat Mass Trans., vol. 3, 1961, pp. 77-83.
7. Mizushina, Tokuro; and Sasano, Tadahisa: The Ratio of the Eddy Diffusivities for Heat and Momentum and Its Effect on Liquid Metal Heat Transfer Coefficients. International Development in Heat Transfer, ASME, 1963, pp. 662-668.
8. Deissler, Robert G. : Turbulent Heat Transfer and Temperature Fluctuations in a Field with Uniform Velocity and Temperature Gradients. Int. Heat Mass Trans., vol. 6, Apr. 1963, pp. 257-270.
9. Dwyer, O. E. : Eddy Transport in Liquid-Metal Heat Transfer. AIChE J., vol. 9, no. 2, Mar. 1963, pp. 261-268.
10. Sesonke, Alexander; Schrock, S. L. ; and Buyco, E. H. : Eddy Diffusivity Ratios for Mercury Flowing in a Tube. AIChE Chem. Engr. Progr. Symp. Ser., vol. 61, no. 57, 1965, pp. 101-107.
11. Schneider, P. J. : Effect of Axial Fluid Conduction on Heat Transfer in the Entrance Regions of Parallel Plates and Tubes. ASME Trans., vol. 79, no. 4, May 1957, pp. 765-773.
12. Martinelli, R. C. : Heat Transfer to Molten Metals. ASME Trans., vol. 69, no. 8, Nov. 1947, pp. 947-959.
13. Dwyer, O. E. : Heat Transfer to Liquid Metals Flowing Turbulently Between Parallel Plates. Nucl. Sci. Engr., vol. 21, no. 1, Jan. 1965, pp. 79-89.

14. Harrison, W. B.; and Menke, J. R.: Heat Transfer to Liquid Metals Flowing in Asymmetrically Heated Channels. ASME Trans., vol. 71, no. 7, Oct. 1949, pp. 797-803.
15. Seban, R. A.: Heat Transfer to a Fluid Flowing Turbulently Between Parallel Walls with Asymmetric Wall Temperatures. ASME Trans., vol. 72, no. 6, Aug. 1950, pp. 789-795.
16. Vary, A.: Electrodynamic Mercury Pump. NASA TN D-2965, 1965.
17. Elliott, D.; Cerini, D.; Eddington, R.; Hays, L.; and Weinberg, E.: Liquid MHD Power Conversion. Space Programs Summary no. 37-33, vol. IV, Jet Propulsion Lab., Calif. Inst. Tech., June 30, 1965, pp. 142-150.
18. Elliott, David G.: Direct Current Liquid-Metal Magnetohydrodynamic Power Generation. AIAA J., vol. 4, no. 4, Apr. 1966, pp. 627-634.
19. Abramowitz, Milton; and Stegun, Irene A.: Handbook of Mathematical Functions with Formulas, Graphs, and Mathematical Tables. NBS, Appl. Math. Ser. 55, June 1964 (3rd printing, Mar. 1965), p. 415.
20. Kutateladze, Samson S.: Fundamentals of Heat Transfer. 2nd rev. ed., Academic Press, Inc., 1963, pp. 217-220.

"The aeronautical and space activities of the United States shall be conducted so as to contribute . . . to the expansion of human knowledge of phenomena in the atmosphere and space. The Administration shall provide for the widest practicable and appropriate dissemination of information concerning its activities and the results thereof."

—NATIONAL AERONAUTICS AND SPACE ACT OF 1958

NASA SCIENTIFIC AND TECHNICAL PUBLICATIONS

TECHNICAL REPORTS: Scientific and technical information considered important, complete, and a lasting contribution to existing knowledge.

TECHNICAL NOTES: Information less broad in scope but nevertheless of importance as a contribution to existing knowledge.

TECHNICAL MEMORANDUMS: Information receiving limited distribution because of preliminary data, security classification, or other reasons.

CONTRACTOR REPORTS: Technical information generated in connection with a NASA contract or grant and released under NASA auspices.

TECHNICAL TRANSLATIONS: Information published in a foreign language considered to merit NASA distribution in English.

TECHNICAL REPRINTS: Information derived from NASA activities and initially published in the form of journal articles.

SPECIAL PUBLICATIONS: Information derived from or of value to NASA activities but not necessarily reporting the results of individual NASA-programmed scientific efforts. Publications include conference proceedings, monographs, data compilations, handbooks, sourcebooks, and special bibliographies.

Details on the availability of these publications may be obtained from:

SCIENTIFIC AND TECHNICAL INFORMATION DIVISION
NATIONAL AERONAUTICS AND SPACE ADMINISTRATION
Washington, D.C. 20546